A STUDY OF PNEUMATIC CAPACITORS

by

Jona Dagan

A

DISSERTATION

in the

FACULTY OF ENGINEERING

Presented in partial fulfilment of the requirements for the

Degree of MASTER OF ENGINEERING

at

Sir George Williams University

Montreal, Canada

March, 1971

Jona Dagan

A STUDY OF PNEUMATIC CAPACITORS

ABSTRACT

Analytical models of charging and discharging of constant and variable volume capacitors, when connected to fluid amplifiers of known operational characteristics, were developed. With these models, the pressure-time characteristics of capacitors can be predicted, provided the polytropic index of the process is determined. Experimental investigations of charging and discharging of constant pneumatic capacitors were conducted. By comparing the experimental and theoretical results, the proper polytropic index for charging and discharging processes can be established. The results indicate that these processes follow very closely the adiabatic process in their initial stages, subsequently tapering off towards isothermal characteristics.

The techniques developed in this investigation are useful in predicting time-delay and design of oscillatory circuits for practical applications.

ACKNOWLEDGEMENTS

I am grateful to Dr. C.K. Kwok, my advisor, for his continuing guidance, his numerous suggestions and his very helpful criticism.

I am also thankful to Mr. N. Suresh and Mr. M. Dalby for their help in performing the experimental work.

This project was supported by the National Research Council of Canada under grant No. A7435.

Jona Dagan

TABLE OF CONTENTS

page

LIST OF TABLES

LIST OF FIGURES

NOMENCLATURE

A	constant, $cfm/psia^2$
A_{eq}	orifice equivalent area, in^2
A_{eq_1}	fluid amplifier "load line" restriction equivalent area, in^2
A_{eq_2}	fluid amplifier "reverse flow" restriction equivalent area, in^2
B	constant, cfm/psia
C	constant, cfm
D	diameter, in.
g	acceleration due to gravity ($g = 32.2$), ft $lbm/sec^2 lbf$
K	spring constant of bellows, lbf/in
k	ratio of specific heats ($k = 1.4$ for air)
L	length, in.
m	mass, lbm
$\dot{m}$	net mass flow rate into capacitor, lbm/sec
$\dot{m}_1$	influx mass flow rate, lbm/sec
$\dot{m}_2$	efflux mass flow rate, lbm/sec
$\dot{m}'$	mass flow rate orifice, lbm/sec
n	polytropic index
P	absolute pressure, psia
P_g	gauge pressure, psig
P_∞	ambient pressure, psia

P_s	amplifier supply pressure, psig
P_1	final pressure in chamber, psia
P_2	initial pressure in chamber, psia
Q_∞	volumetric flow rate at ambient pressure and temperature conditions, scfm
R	gas constant for air (R = 53.3), lbf ft/lbm°R
S	equivalent cross-section area of bellows, in^2
T	temperature, °R
T_∞	ambient temperature, °R
T_1	final temperature in chamber, °R
t	time variable, sec
V	volume, in^3
V_o	constant volume, in^3
X	linear displacement of bellows, in.
ρ	mass density of air, lbm/in^3
ρ_∞	ambient mass density, lbm/in^3
$\bar{\rho}$	average mass density in chamber, lbm/in^3

CHAPTER 1

INTRODUCTION

Recent trends towards the use of fluidic control sub-systems in the design of industrial pneumatic systems have pointed out the necessity for a better understanding of the interactions between fluid amplifiers and passive fluid circuit elements, such as resistors and capacitors.

Fluidic capacitors, in particular, have been widely employed in the construction of oscillators and time delays for use in industrial control systems. Despite such wide usage, the literature on fluidic capacitors and their interaction with other active elements is very limited.

Early in 1951, Ahrendt and Taplin [1] derived approximate values for the pneumatic capacitance of a fixed mass of air for simple isothermal and ideal isentropic compressions. The analytical results are applicable for pressure variation only in the order of 2.5% of the mean pressure. Helm [2] discussed some aspects of the pneumatic capacitance with variable volumes. Zalmonson [3,4] in 1965 presented probably one of the most extensive studies of pneumatic capacitance covering detailed investigations of steady state and transient conditions

of charging and discharging phenomena of pneumatic capacitors. Most of the analytical treatments were carried out on cases where isothermal flow conditions were assumed. Extensive experimental data were used to substantiate the theoretical work.

Letham [5], in a special publication of Machine Design, attempted to use electrical analogy to derive expressions for pneumatic capacitors. A similar approach was followed by Kirshner [6], Woodson [7] and Humphrey and Manion [8]. The derived equivalent expressions for pneumatic capacitance greatly simplify the circuit design procedure. However, special caution must be exercised during application because the highly non-linear characteristics of real fluid flow result, in some cases, in a significant departure from the exact electrical analogy.

Hind and Hahn [9] attempted to develop the transfer function of the pneumatic capacitance of a fixed mass of gas enclosed in a rigid container, taking into account pressure variations caused by heat transfer during both the compression and expansion processes. After certain simplifying assumptions, the transfer function was shown to be related solely to the polytropic index of compression. Volume-flow approach was used

for that study. However, some other authors prefer the mass-flow approach, especially for cases where actual mass flow of air is involved in the charging and discharging processes. Taplin and Seleno [10] developed yet another electrical analogy for pneumatic capacitors using the mass-flow concept. A new voltage drop equivalent in the form RT $\ln\left(\frac{P(final)}{P(initial)}\right)$ was derived where P, T and R are pressure, temperature and gas constant for the fluid, respectively.

Anderson [11] analyzed the static and dynamic characteristics of both fixed and variable volume capacitors. The results, in a way similar to those presented by Hind and Hahn, indicated that the process of charging and discharging of pneumatic capacitors depends on the polytropic index "n". No experimental data were presented to show the value of "n" in actual circuit applications.

In an attempt to gain better insight into the actual charging and discharging mechanism in pneumatic capacitors, and to obtain the proper value of "n" which can be used in actual pneumatic circuits, the present theoretical and experimental studies were carried out.

It is important that the exact mechanism of charging

and discharging of capacitors be understood; therefore, it is not intended to use the electrical analogy approach in the development of capacitance relationships. Instead, the whole analysis will be carried out purely from the basic thermodynamic and fluid mechanics point of view. The main objectives are defined as follows:

(1) to develop analytical expressions for charging and discharging of constant and variable volume fluid capacitors when connected to fluid amplifiers of known operational characteristics;

(2) to experimentally investigate the charging and discharging processes of constant volume capacitors;

(3) to compare the experimental and analytical results and establish the actual index of polytropic process "n".

CHAPTER 2

THEORETICAL ANALYSIS

2.1 General

A common way of analyzing fluidic systems, as mentioned in the previous chapter, is by using electrical analogy. However, the non-linear characteristics, which are unique to fluids, render the analogy inapplicable in many practical cases. Since there are difficulties in defining exact yet meaningful electrical/fluid analogies, many investigators have derived different analogies to suit their own particular systems. A list of these analogies is given in Table I.

The existence of such a variety of electrical/fluid analogies may sometimes cause confusion even to people who are experienced in the field. Therefore in some cases it is easier to analyze the system purely by making use of the thermodynamic and fluid mechanics theories. This approach was adopted for the following analysis of the charging and discharging of pneumatic capacitors.

2.2 Charging and Discharging Processes of Pneumatic Capacitors

2.2.1. Description of pneumatic capacitors

Pneumatic capacitors basically consist of a chamber with one or more input-output ports. Such chambers belong either to the fixed volume type (capacitors), such as gas cylinders, or to the variable volume type (capacitors) such as bellows or balloons, as shown in Fig. 1.

In fixed volume capacitors, the capacitance effect depends entirely on the compressibility of the gas, whereas in variable volume capacitors, both the elastic properties of the chamber and the compressibility of the gas affect the overall capacitance. Both constant and variable volume capacitors will be considered in the present study.

For the development of a general theory for charging and discharging pneumatic capacitors, a volume with an input and an output port is considered. During charging, fluid will be admitted through the input port, and at the same time vented through the output port. When the input flow terminates and the discharging mode takes place, fluid will be vented through both ports simultaneously. This seemingly simple mode can actually be used to represent the most general case. For

example, volumes with any number of input-output ports can be transformed into volumes with two equivalent input and output ports.

A pneumatic capacitor is a passive device which does not require power supply but is capable of modulating input signals in the manner characteristic of the element. Typical applications of pneumatic capacitors in fluidic time delay circuits are shown in Figs. 2a and 2b. In both circuits, it can be seen that when the capacitor is charged through the output leg of the active amplifier, partial discharge is taking place through the output port. The output port is connected to the control port of the amplifier itself or to other compatible elements. In order for the pressure to build up within the capacitor, the in-flow rate must be larger than the total out-flow. When the input fluid is suddenly terminated (i.e. when the fluid amplifier is switched to the alternate output leg), the capacitor leaks out through both the input and output ports. It may be advantageous to note at this point that during discharge, the accumulated flow which discharges through the input port and flows back via the output leg of the fluid amplifier is termed the "reverse flow".

2.2.2. Development of mathematical relationships

2.2.2.1. The fluid amplifier characteristics: For the analysis of the charging and discharging processes of pneumatic capacitors, the following characteristics of the fluid amplifiers must first be known:

(1) the output characteristics of the amplifier;

(2) the pressure-flow characteristics of the amplifier control port. These are sometimes known as the load line characteristics;

(3) the "reverse flow" characteristics of the amplifier.

Typical curves of the above-mentioned characteristics are sketched in Fig. 3. The output characteristics of the fluid amplifiers are usually supplied by its manufacturer. A sample data sheet of the Aviation Electric monostable amplifier, which was used in the later experimental studies, is given in Appendix I. These characteristics were also determined experimentally in order to verify the accuracy of the manufacturer's data. Using standard curve-fitting techniques, the amplifier's output characteristic curves can be represented by quadratic polynomial equations with appropriate constants. The general

equation of such polynomials can be expressed as:

$$Q_\infty = AP^2 + BP + C \tag{1}$$

where A, B and C are constants, and P and Q_∞ are pressure and flow rate respectively.

The "load line" and "reverse flow" characteristics can also be determined experimentally and will be shown later. Instead of using the similar curve-fitting techniques, as for the output pressure-flow characteristics, another method was devised by comparing the experimental curves with actual orifice flow characteristics. In other words, "load line" and "reverse flow" characteristics of a particular amplifier may be considered equivalent to orifices of finite sizes. In order to compute standard orifice flow characteristics, the equations derived in Shapiro [13] for isentropic flow of a perfect gas were used. For subsonic flow, which is generally encountered in fluid circuits, the relation of mass flow rate to an orifice of equivalent area "A_{eq}" may be expressed as:

$$\dot{m}' = \frac{A_{eq} P}{\sqrt{RT_\infty}} \sqrt{\frac{2kg}{(k-1)} \left[\left[\frac{P_\infty}{P}\right]^{k+1/k} - \left[\frac{P_\infty}{P}\right]^2 \right]} \tag{2}$$

where k = 1.4 is the ratio of specific heats of air, and all the

other symbols are defined in the nomenclature.

In special cases, when the pressure ratio (P_∞/P) across the orifice decreases beyond the critical ratio (i.e. $(P_\infty/P)_{crit}$ = 0.528 at k = 1.4), supersonic flow occurs. The mass flow rate is then given by

$$\dot{m}' = A_{eq}\sqrt{\frac{kg}{RT_\infty}}\left(\frac{2}{k+1}\right)^{k+1/2(k-1)} P_\infty^{\,k-1/k}\, P^{1/k} \qquad (3)$$

For known equivalent orifice areas "A_{eq}", and atmospheric conditions, eqs. (2) and (3) can be used to compute the pressure-flow characteristics. These curves were obtained analytically for various equivalent areas, and are plotted in Fig. 4. By simply comparing these analytical curves of different orifice areas with the amplifier "load line" and "reverse flow" characteristics, it may be possible to select appropriate orifice pressure-flow curves to represent the amplifier characteristics mentioned above. This is also indicated in Fig. 4.

2.2.2.2. Charging process of constant volume pneumatic capacitors: As previously described, during the charging process, air is entering the capacitor from the output leg of one amplifier and at the same time a certain amount

of air is leaking out through the control port of another amplifier, as shown in Fig. 2a. In the development of an analytical model for charging and discharging the capacitor, the following assumptions are made:

(1) air behaves as an ideal gas (i.e. $P = \rho RT$);

(2) a polytropic process takes place (i.e. P/ρ^n = constant); the index of the polytropic process "n" lies between n = 1 for isothermal processes and n = 1.4 for adiabatic processes;

(3) the instantaneous pressure and temperature are uniform at all points within the capacitor volume;

(4) the pressure rise in the capacitor is independent of the geometric configuration of the volume.

For the polytropic process:

$$\frac{P}{\rho^n} = \frac{P_\infty}{\rho_\infty^n} = \text{constant} \qquad (4)$$

Differentiating eq. (4), one obtains,

$$dP = \frac{nP}{\rho} d\rho \tag{5}$$

Since $m = \rho V$, where V is the volume of the capacitor and m is the mass enclosed in this volume, the instantaneous net mass flow rate "$\dot{m}$" into the capacitor becomes:

$$\dot{m} = \rho \frac{dV}{dt} + V \frac{d\rho}{dt} \tag{6}$$

For the case where constant volume is considered, $dV/dt = 0$.

$$\therefore \dot{m} = V_o \frac{d\rho}{dt} \tag{7}$$

where V_o is the volume of the capacitor for the case of constant volume.

From eqs. (4), (5) and (7)

$$\dot{m} = \frac{V_o \rho}{nP} \frac{dP}{dt} = \frac{V_o \rho_\infty}{nP_\infty^{1/n}} P^{1-n/n} \frac{dP}{dt} \tag{8}$$

Making a mass flow balance of the flows into and out of the capacitors, one obtains

$$\dot{m} = \dot{m}_1 - \dot{m}_2 \tag{9}$$

where $\dot{m}_1$ is the mass flow rate into the capacitor from the output of the charging amplifier, and can be expressed using eq. (1) as follows:

$$\dot{m}_1 = \rho_\infty (AP^2 + BP + C)\, 28.8 \tag{10}$$

where 28.8 is a unit conversion factor, $in^3 min/ft^3 sec$. $\dot{m}_2$ is the mass flow rate out of the capacitor through the control port of the loading amplifier. Its magnitude can be expressed by using eqs. (2) or (3) depending on whether the flow is subsonic or supersonic. The equivalent area is found by comparing the actual characteristics with orifice pressure-flow curves shown in Fig. 4. Substituting the mathematical expressions for $\dot{m}$, $\dot{m}_1$, and $\dot{m}_2$ into eq. (9), the following two equations are obtained:

For subsonic flow:

$$\frac{dP}{dt} = \frac{nP_\infty^{1/n}}{V_o} P^{n-1/n} \left\{ (AP^2 + BP + C)\, 28.8 - \frac{A_{eq_1} P}{\rho_\infty \sqrt{RT_\infty}} \sqrt{\frac{2kg}{(k-1)} \left[\left(\frac{P_\infty}{P} \right)^{k+1/k} - \left(\frac{P_\infty}{P} \right)^2 \right]} \right\} \tag{11}$$

and for supersonic flow:

$$\frac{dP}{dt} = \frac{nP_{\infty}^{1/n}}{V_o} P^{n-1/n} \left\{ (AP^2 + BP + C)\,28.8 \right.$$

$$\left. - \frac{A_{eq_1}}{\rho_{\infty}} \sqrt{\frac{kg}{RT_{\infty}}} \left(\frac{2}{k+1}\right)^{k+1/2(k-1)} P_{\infty}^{k-1/k} P^{1/k} \right\} \qquad (12)$$

Applying the initial conditions at $t = 0$, $P = P_{\infty}$, the instantaneous pressure "P" in the capacitor during the charging period can be determined. However, because it is difficult to solve these equations analytically, a numerical solution was sought. A computer programme was prepared using the Runge-Kutta method for solving these differential equations. A sample programme is presented in Appendix II.

2.2.2.3. Discharging process of constant volume pneumatic capacitor: During the discharging mode of the capacitors, accumulated air in the volume is vented through both the inlet and outlet ports. Since the input flow terminates during the discharge, $\dot{m}_1 = 0$. The mass flow rate leaving the capacitor "$\dot{m}_2$" is determined by either eqs. (2) or (3), depending on whether the flow is supersonic or subsonic. Total equivalent area for the "load line" and "reverse flow" characteristics may be expressed as:

$$A_{eq} = A_{eq_1} + A_{eq_2} \tag{13}$$

where A_{eq_1} and A_{eq_2} are obtained from Fig. 4.

Similar to the charging process, the differential equations for the instantaneous pressure within the capacitor may be obtained as follows:

For subsonic flow:

$$\frac{dP}{dt} = - \frac{nP_\infty^{1/n}(A_{eq_1} + A_{eq_2})}{V_o \rho_\infty \sqrt{RT_\infty}} P^{2n-1/n} \sqrt{\frac{2kg}{(k-1)}\left[\left(\frac{P_\infty}{P}\right)^{k-1/k} - \left(\frac{P_\infty}{P}\right)^2\right]} \tag{14}$$

and for supersonic flow:

$$\frac{dP}{dt} = - \frac{nP_\infty^{1/n}(A_{eq_1} + A_{eq_2})}{V_o \rho_\infty} \sqrt{\frac{kg}{RT_\infty}}\left(\frac{2}{k+1}\right)^{k+1/2(k-1)} P_\infty^{k-1/k} P^{(\frac{1}{k}+\frac{n-1}{n})} \tag{15}$$

The initial pressure for the discharge is actually the maximum pressure attained during the charging process. Again, eqs. (14) and (15) may be solved numerically by the Runge-Kutta method.

2.2.2.4. Charging and discharging processes of variable volume pneumatic capacitors: The variable volume which will be considered here is of the bellows type, as shown in Fig. 1. This type of variable volume capacitor is commonly used in pneumatic control systems.

The assumptions used for the development of the analytical model of the variable volume capacitor are summarized as follows:

(1) air behaves as an ideal gas (i.e. $P = \rho RT$);

(2) a polytropic process takes place (i.e. P/ρ^n = constant); the index of polytropic process "n" lies between n = 1 for isothermal processes and n = 1.4 for adiabatic processes;

(3) the instantaneous pressure and temperature are uniform at all points within the capacitor volume;

(4) the pressure rise in the capacitor is independent of the geometric configuration of the volume;

(5) effects of the mass acceleration of the moving parts are

negligible.

(6) friction forces are negligible.

In order to determine the differential equations for the charging and discharging of a variable volume capacitor, it is necessary to know $\dot{m}$, $\dot{m}_1$ and $\dot{m}_2$. $\dot{m}_1$ and $\dot{m}_2$ are independent of the volume variations, but they are dependent on the instantaneous pressure within the volume, as well as on the characteristics of both the driving and loading fluid amplifiers. Thus, the equations for $\dot{m}_1$ and $\dot{m}_2$ are the same as those of the constant volume charging and discharging processes. However, $\dot{m}$ is a function of both the instantaneous density and the variable volume "V", as shown in eq. (6):

$$\dot{m} = \rho \frac{dV}{dt} + V \frac{d\rho}{dt} \tag{6}$$

In order to find V as a function of P, the bellows equations must be considered. Using the simple relationship for bellows:

$$P_g S = KX \tag{16}$$

where S and K are the equivalent cross-sectional area, and the spring constant of the bellows respectively, and X is the linear displacement of the bellows.

From Fig. 1, it can be seen that:

$$V = V_o + SX \tag{17}$$

Combining eqs. (16) and (17)

$$V = V_o + \frac{S^2}{K} P_g = V_o + \frac{S^2}{K}(P - P_\infty) \tag{18}$$

Differentiating eq. (18), one obtains:

$$dV = \frac{S^2}{K} dP \tag{19}$$

Substituting the expressions for V and dV from eqs. (18) and (19) into eq. (6), it can be shown that:

$$\dot{m} = \left[\frac{\rho S^2[(n+1)P - P_\infty]}{KnP} + \frac{V_o \rho}{nP}\right]\frac{dP}{dt} \tag{20}$$

The first term in this equation represents the effect of variation of the volume on $\dot{m}$. If K is very small, the first term predominates. From a physical point of view, this means that volume change is very large and the effect due to the second term $(V_o\rho/nP)dP/dt$ is negligible. The opposite holds true when K becomes large.

Having obtained the expression for $\dot{m}$, and using the same procedure as for the constant volume analysis to obtain $\dot{m}_1$ and $\dot{m}_2$, the following set of differential equations are obtained:

1) For charging of a variable volume capacitor under:

Subsonic Flow Conditions

$$\frac{dP}{dt} = \frac{KnP_\infty^{1/n}}{[(n+1)S^2P - S^2P_\infty + V_oK]} P^{n-1/n}\left\{(AP^2+BP+C)\,28.8 - \frac{A_{eq_1}P}{\rho_\infty\sqrt{RT_\infty}}\sqrt{\frac{2kg}{(k-1)}\left[\left(\frac{P_\infty}{P}\right)^{k+1/k} - \left(\frac{P_\infty}{P}\right)^2\right]}\right\} \qquad (21)$$

Supersonic Flow Conditions

$$\frac{dP}{dt} = \frac{KnP_\infty^{1/n}}{[(n+1)S^2P - S^2P_\infty + V_oK]} P^{n-1/n}\left\{(AP^2+BP+C)\,28.8 - \frac{A_{eq_1}}{\rho_\infty}\sqrt{\frac{kg}{RT_\infty}}\left(\frac{2}{k+1}\right)^{k+1/2(k-1)} P_\infty^{k-1/k}\,P^{1/k}\right\} \qquad (22)$$

2) For discharging of a variable volume capacitor under:

Subsonic flow conditions

$$\frac{dP}{dt} = - \frac{nKP_{\infty}^{1/n}(A_{eq_1} + A_{eq_2})}{\rho_{\infty}[(n+1)S^2P - S^2P_{\infty} + V_oK]\sqrt{RT_{\infty}}} P^{2n-1/n} \sqrt{\frac{2kg}{(k-1)}\left[\left(\frac{P_{\infty}}{P}\right)^{k-1/k} - \left(\frac{P_{\infty}}{P}\right)^{2}\right]} \tag{23}$$

Supersonic flow conditions

$$\frac{dP}{dt} = - \frac{nKP_{\infty}^{1/n}(A_{eq_1} + A_{eq_2})}{\rho_{\infty}[(n+1)S^2P - S^2P_{\infty} + V_oK]} \sqrt{\frac{kg}{RT_{\infty}}}\left(\frac{2}{k+1}\right)^{k+1/2(k-1)} P_{\infty}^{k-1/k} P^{(\frac{1}{k}+\frac{n-1}{n})} \tag{24}$$

The solutions of eqs. (21) through (24) may be obtained by using numerical methods similar to those described in Section 2.2.2.2. and Appendix II.

CHAPTER 3

EXPERIMENTS

3.1 General

A series of experiments was designed to check the validity of the analytical relationships derived for constant volume capacitors. It is hoped that by comparing the experimental results with theoretical data a better insight may be achieved regarding the thermodynamic processes which take place during charging and discharging of the capacitor.

3.2 Experimental Set-Up

The general experimental set-up is shown schematically in Fig. 5. Studies were conducted on the charging and discharging phenomena of eleven pneumatic capacitors with different geometric configurations. These are tabulated in Table 2. The charging process was carried out by connecting the output 01, which is normally active, of an Aviation Electric Monostable amplifier AE 1100M01, to the capacitor input port. The reason

for using 01 output port rather than 02 is to eliminate the possible error involved due to the additional flow rate of the control input. It can be seen from the schematic diagram in Fig. 5 that the on-off switch connected in parallel to the power supply flow is normally "on". When the switch is depressed, the control jet supply pressure is off and the output of the monostable amplifier switches immediately from 02 to 01. Charging of the capacitor takes place.

The upper control port C1 of another, similar monostable amplifier, operating at the same supply pressure as that of the charging amplifier was connected to the pneumatic capacitor output port. Each capacitor was charged and discharged by the amplifiers with supply pressures of 2.5, 5, 7.5 and 10 psig.

The pressure variations within the chamber were measured by a Pace-Wiancko differential pressure transducer system No. KP15-CP25. The transducer used has a cavity volume, according to the manufacturer's specifications, of only 0.004 in^3. This is less than 0.1% of the smallest chamber considered. Therefore, the effect of the transducer volume may be considered to be negligible. The dynamic response of the transducer is

quoted to be up to 1000 Hertz. The minimum time constant for charging and discharging the smallest volume was initially predicted to be in the range of 0.01 second. Therefore, this transducer is considered adequate for the present investigation. Output of the transducer system was fed directly to a Brush Mark 280 strip chart recorder with chart drive speed of 100 mm/sec.

Static calibration for the transducer was carried out according to the procedure recommended by the manufacturer. Results are presented in Fig. 6.

CHAPTER 4

RESULTS AND CONCLUSIONS

4.1 Presentation of Results

The experimental results for the charging and discharging characteristics of different volumes at various values of supply pressures were recorded by using a strip chart recorder. These accurately reproduced results are shown in Figs. 7 to 17.

The theoretical pressure rise and drop rates for charging and discharging of the capacitors were obtained numerically (as shown in Appendix II) by solving eqs. (11) and (12) for the charging, and eqs. (14) and (15) for the discharging processes. In order to be able to solve the above-mentioned equations, it was necessary first to obtain the constants A, B, C, A_{eq_1} and A_{eq_2} which define the operational characteristics of the fluid amplifiers. These constants were obtained experimentally as described in Appendix III. In general, some of these functions can be obtained from manufacturers of fluid amplifiers. In addition, the initial pressure conditions in the capacitor must be known.

As stated previously, the initial pressure in the chamber for the charging process was "P_∞", and for the discharging process it was the maximum pressure attained in the capacitor during the charging process. The volume "V_o" was chosen to be the same as the experimentally investigated volumes, varying from 5-15 in^3 in 5 in^3 increments.

Once these parameters are defined, the only unknown constant occurring in these equations is n, the polytropic index. The adiabatic case where n = 1.4, and the isothermal case where n = 1.0, represent the two extreme cases for "n" related to charging and discharging of the pneumatic chamber. These two cases were used for the numerical solution of the above equations.

4.2 Discussion of Results

As the experiments were conducted in three different volumes of 5, 10 and 15 in^3, the results can be grouped accordingly. Thus group No. 1 will include all the volumes of 5 in^3 (Figs. 7-10), group No. 2 all the volumes of 10 in^3 (Figs. 11-14), and group No. 3, the volumes of 15 in^3 (Figs. 15-17).

First, by comparison of the results within each group of chambers, it is seen that for the same chamber volume with different diameter-to-length ratios, almost identical experimental results are obtained. This result is very important as it verifies the basic assumption undertaken in the theoretical analysis of pneumatic capacitors that the pressure-time characteristics during charging and discharging are not a function of the geometric configuration of the chamber. This may be true for the present experimental investigation because the pressure levels involved are quite low. However, it is suspected that with increasing pressure and flow rate during the charging process, a significant departure of experimental results between chambers of different geometries and input-output port arrangements may occur.

The experimental and theoretical results for group No. 1, of 5 in^3 volumes, are shown in Figs. 7-10. For the lower amplifier supply pressures of 2.5 and 5 psig, the actual process follows very closely the theoretical adiabatic process, until the pressure in the capacitor rises to about 75% of its maximum value. At this point the actual process starts to deviate from the adiabatic process and slowly approaches the isothermal process. Similarly, for the higher amplifier supply pressures

of 7.5 and 10 psig, the actual process closely follows the adiabatic process during the initial period of charging. However, at these supply pressures, the actual process already starts to deviate towards the isothermal process in the vicinity of 40% of the maximum pressure. This finding is very interesting and may be interpreted in the following manner. During the initial stage of charging, the flow rate into the chamber and the pressure build-up within the capacitor are quite rapid. Since the in-flowing air has gone through an expansion process with temperature drop, there is really not sufficient time for heat transfer to take place. As a result, the flow process resembles an adiabatic one with "n" equal to 1.4. As pressure in the pneumatic capacitor is gradually building up, it can be seen from the output characteristics of the fluidic amplifier that the flow rate into the chamber is also reduced. In other words, the rate of charging is also decreased. When the charging rate is slow, sufficient time is allowed for heat transfer to take place and the process gradually resembles that of an isothermal case where "n" equals 1.

In most practical applications where capacitors are used to create time delay for building up pressure levels, the desired pressure level is usually below 63.2% of the maximum

attainable level of the chamber. This general rule is to ensure repeatability of the time delay circuit by confining the operation within a region where a well-defined pressure-time characteristic is repeatedly obtainable. Therefore, it follows from the results that the adiabatic process may be considered for predicting charging processes of capacitors for practical circuit design.

In the initial time period of the discharge process, at any of the supply pressure conditions, both the theoretical isothermal and adiabatic processes follow very closely the actual processes. It is only in the final phase of discharging that the actual process tends to move towards the isothermal case when n equals 1. As mentioned previously, discharge starts when the pneumatic chamber has reached its maximum pressure. When this happens, sufficient time has been allowed for heat transfer to take place and the temperature of the accumulated air in the chamber is almost equal to that of the ambient. Because of the size of the volume, it may be considered that most of the discharge takes place with air in the chamber remaining almost constant, with very little heat transfer taking place since the temperature gradient between the air inside the chamber and the environment is small. Consequently, the theoretical curves for the adiabatic and isothermal cases are very close to

each other. For all practical purposes, either adiabatic or isothermal cases may be used for prediction of the discharge characteristics without introducing too great an error.

From Figs. 7-10, it can be seen that except for the experimental data taken at an amplifier supply pressure of 2.5 psig, all the maximum pressures reached in the capacitor correspond very well with the theoretical curves calculated based on either isothermal or adiabatic cases. The reason for the discrepancy for the case of the lowest supply pressure may be traced back to the error in curve fitting as shown in Fig. A.2. The maximum pressures recovered for cases of 5, 7.5 and 10 psig are matched very well with the theoretical curves. However, for the case of 2.5 psig supply pressure, there is a discrepancy of approximately 10% for the value of maximum pressure recovery. This error is reflected in the comparison of the experimental data and theoretical curves which were calculated based on the curves in Fig. A.2.

Group No. 2 experiments were carried out on volumes of 10 in^3. The results are shown in Figs. 11-14 and indicate similar trends to those of the smaller volume. The actual charging process closely follows the theoretical adiabatic process at the initial stages of charging; however, it changes for different

amplifier supply pressures. For the lower supply pressure conditions, 2.5 and 5 psig, when the pressure in the capacitor reaches 60-75% of its maximum, the actual process tends to change slowly towards the isothermal process. For the higher supply pressures, this deviation occurs at pressures of about 30-50% of the maximum.

During discharge, a bigger gap between the theoretical adiabatic and isothermal processes can be noticed. The actual process follows very closely the theoretical adiabatic curve in the beginning of the process. After approximately 60-70% pressure drop, it heads slowly towards the isothermal process. This may be explained by the fact that as the chamber volume is increased, keeping the equivalent discharge orifice constant, then the total time for the discharge will increase. The initial phase of the discharge will resemble the adiabatic process, but eventually when heat transfer starts to take place, the discharge will tend towards the isothermal process.

Group No. 3 involves testing of capacitors of volume equal to 15 in^3 and the results are shown in Figs. 15-17. Similar phenomena to those observed in the two previous groups take place, except that the charging and discharging processes

were taking place over a longer time period. Discrepancies realized for the maximum pressures reached during the charging, as noted from the figures, are due to the fact that not sufficient time was allowed for the complete charging process to take place. If more time is allowed, then the experimental and theoretical curves will eventually meet or become very close to each other. The main object is to compare these results and recognize the type of process actually taking place.

A very useful tool for comparison of various capacitors is known in physical systems as the "time constant". For charging of capacitors, the time constant is defined as the time required to charge the capacitor up to (1 - 1/e), or 63.2% of its maximum capacity. Similarly, for the discharging of capacitors, the time constant is defined as the time required to discharge 63.2% of the capacitor's maximum pressure level. In the following discussion, the time constant term will be used for comparison between the various results. For convenience, all the time constants obtained for charging and discharging are tabulated in Table 3. It is seen from Table 3a that the time constant goes up with increase of volume. This is expected because both the charging amplifier and discharge equivalent area

are kept constant, thus any increase of volume will require additional time for the complete charging process to take place. It is also interesting to note that the time constant for a constant volume goes up with increase of supply pressure. However, the increase is not necessarily a linear relationship. For example, increase of 100% of supply pressure from 5 to 10 psig causes an average increase in time constant of less than 50%. This means that for high supply pressures, the pressure rise rate in the capacitor is actually faster than at low supply pressures. For discharging, the time constant is about half that of the charging process using equivalent areas for the discharge orifice, as described previously. For a constant volume, the time constant for the discharge with a higher initial pressure is longer than that with a lower initial pressure. The time constant is strongly dependent on the volume of the chamber as shown in Table 3b.

It is seen from Figs. 7 to 17 that, for charging, most curves are nearly linear up to pressures of about 63% of maximum, or until the time equals that of the time constant.

As mentioned previously, the pressure value of 63.2%, or the time constant, is generally used as a limit for consideration of charging. Below this limit, linear pressure/time

characteristics can generally be achieved. It follows, therefore, that the values obtained for the time constants and the interrelationships between time constants, amplifier supply pressures and chamber volumes can be most useful for the design of fluidic systems and circuits.

It should be noted that all experimental results presented in this report were obtained based on a particular experimental set-up tested under specific environmental conditions (i.e. room temperature 70°F). The rate of heat transfer during the charging and discharging processes is undoubtedly a function of the environmental temperature. It also depends on the physical properties of the material and the geometric configuration of the chamber. However, the conclusion is drawn that the pressure-time characteristics will follow closely those of the adiabatic process during the initial charging, and the subsequent tapering-off towards the isothermal characteristics will hold for most practical cases.

CONCLUSIONS

Analytical models for charging and discharging of constant as well as variable volume capacitors were developed in conjunction with the operating characteristics of a fluid amplifier. By comparing the theoretical curves, calculated on the basis of different values of the polytropic index, with experimental data, it is possible to establish the proper polytropic index for the actual charging and discharging processes.

The results indicate that for the charging process with a pressure level below 63.2% of the maximum, the adiabatic process of $n = 1.4$ may be used. Similarly for the discharging process, $n = 1.4$ may be considered when the final discharge pressure is greater than 36.8% of the maximum pressure level. When charging and discharging processes are taken beyond the time constant of the pneumatic capacitor, the processes approach the isothermal where $n = 1$.

With known fluid amplifier performance characteristics, it is now possible to use the technique developed here to predict exactly the charging and discharging processes of pneumatic capacitors. This serves to facilitate engineering design of time-delay and oscillating circuits where pneumatic capacitors are used.

TABLE I

Fluid/Electric Analogies

Reference	Current Analog	Voltage Analog	Capacitance
Letham[5]	$\dot{m}$	P	V/nRT
Kirshner[6]	$\dot{m}$	$P/\overline{\rho}$	$\overline{\rho}V/nRT$
Taplin and Seleno[10]	$\dot{m}$	$RT_1 \ell n \left(\frac{P_1}{P_2}\right)$	$PV/k(RT_1)^2$
Krishnaiyer and Lechner[12]	Q	P	V/kP

TABLE II

Physical Dimensions and Volumes

of the Experimental Chambers

No.	Volume (in^3)		Inside dia. (in)	Length (in)	D/L
	Design	Actual			
1	5	5.05	0.875	8.40	0.104
2	5	4.93	1.500	2.80	0.535
3	5	5.16	2.000	1.64	1.240
4	5	4.99	2.500	1.02	2.450
5	10	10.03	0.875	16.70	0.052
6	10	9.80	1.500	5.55	0.270
7	10	10.03	2.000	3.20	0.625
8	10	10.00	2.500	2.04	1.225
9	15	14.70	1.500	8.30	0.181
10	15	14.90	2.000	4.75	0.420
11	15	14.65	2.500	3.00	0.833

NOTE: All the chambers were manufactured from Plexiglas tubing with 0.125" wall thickness.

The coefficient of thermal conductivity of this material is $1.3 \frac{\text{BTU}}{\text{hr. ft}^2\ ^\circ\text{F in.}}$.

TABLE III

Time Constants

(a) Charging: measured time constants in seconds as a function of volume and supply pressures

V (in^3) \ P_s (psig)	2.5	5	7.5	10
5	.04	.05	.06	.07
10	.07	.09	.115	.13
15	.11	.14	.165	.19

(b) Discharging: measured time constants in seconds as a function of volume and supply pressures

V (in^3) \ P_s (psig)	2.5	5	7.5	10
5	.01	.02	.03	.035
10	.04	.05	.065	.075
15	.05	.07	.085	.11

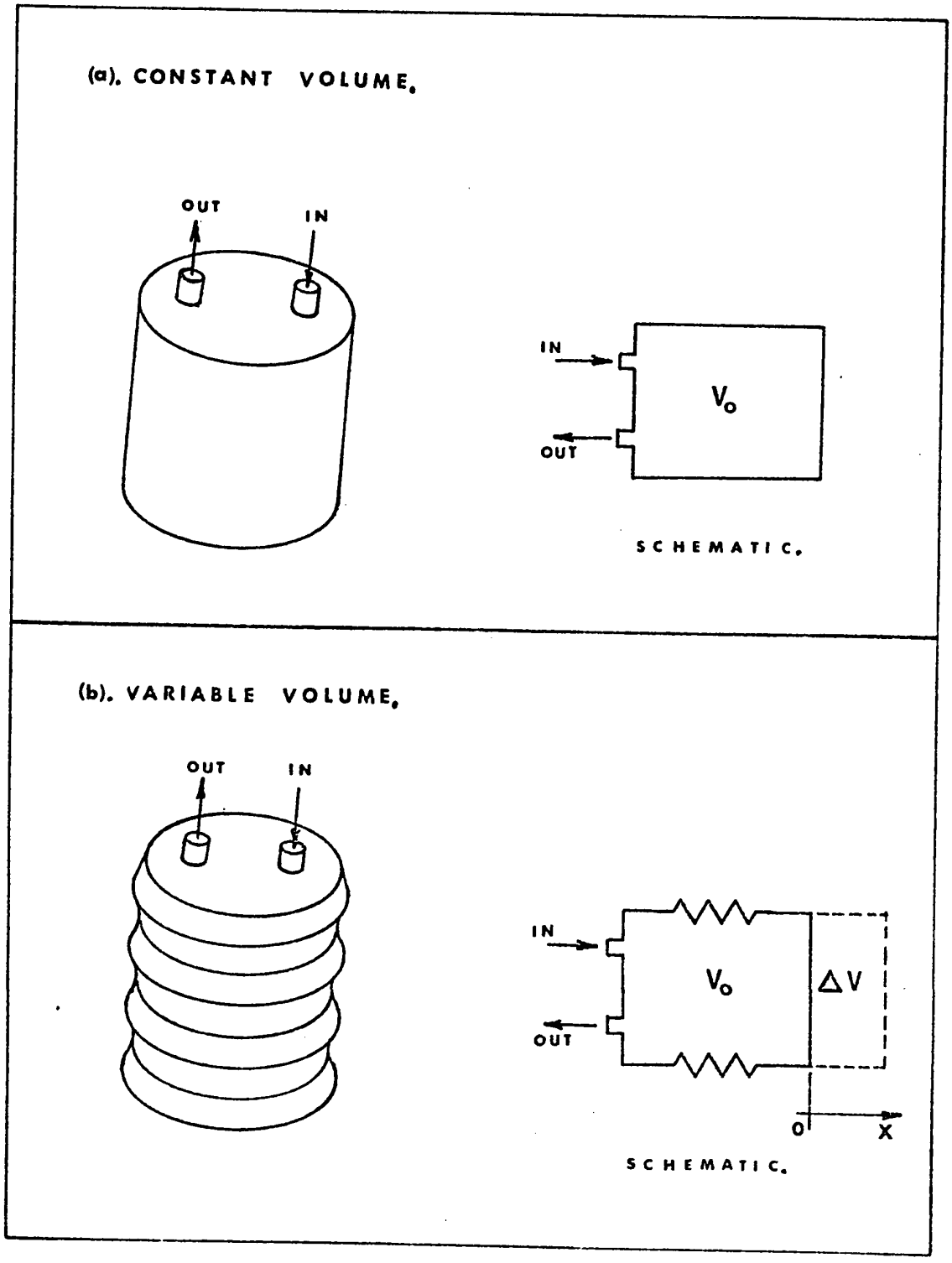

Figure 1. PNEUMATIC CAPACITORS.

(a).

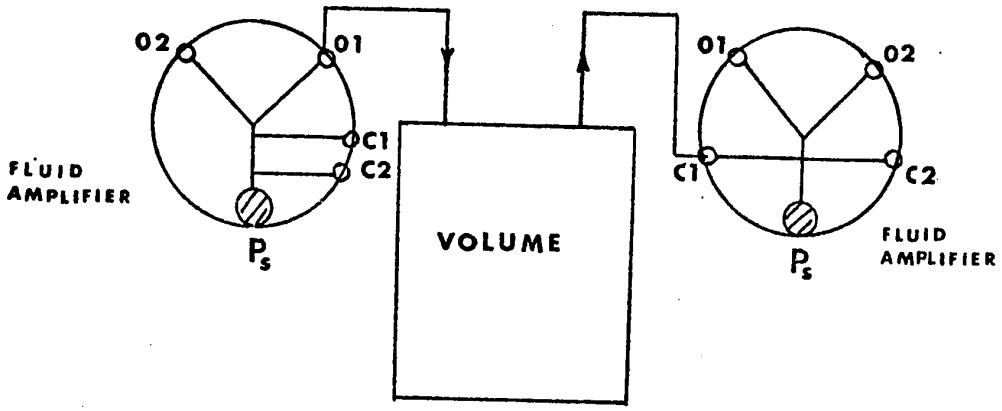

(b).

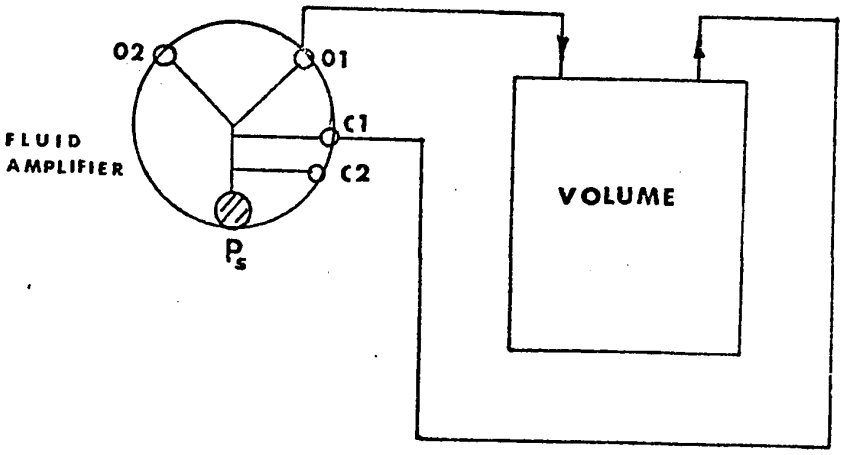

Figure 2. TYPICAL FLUID AMPLIFIER TIME DELAY CIRCUITS.

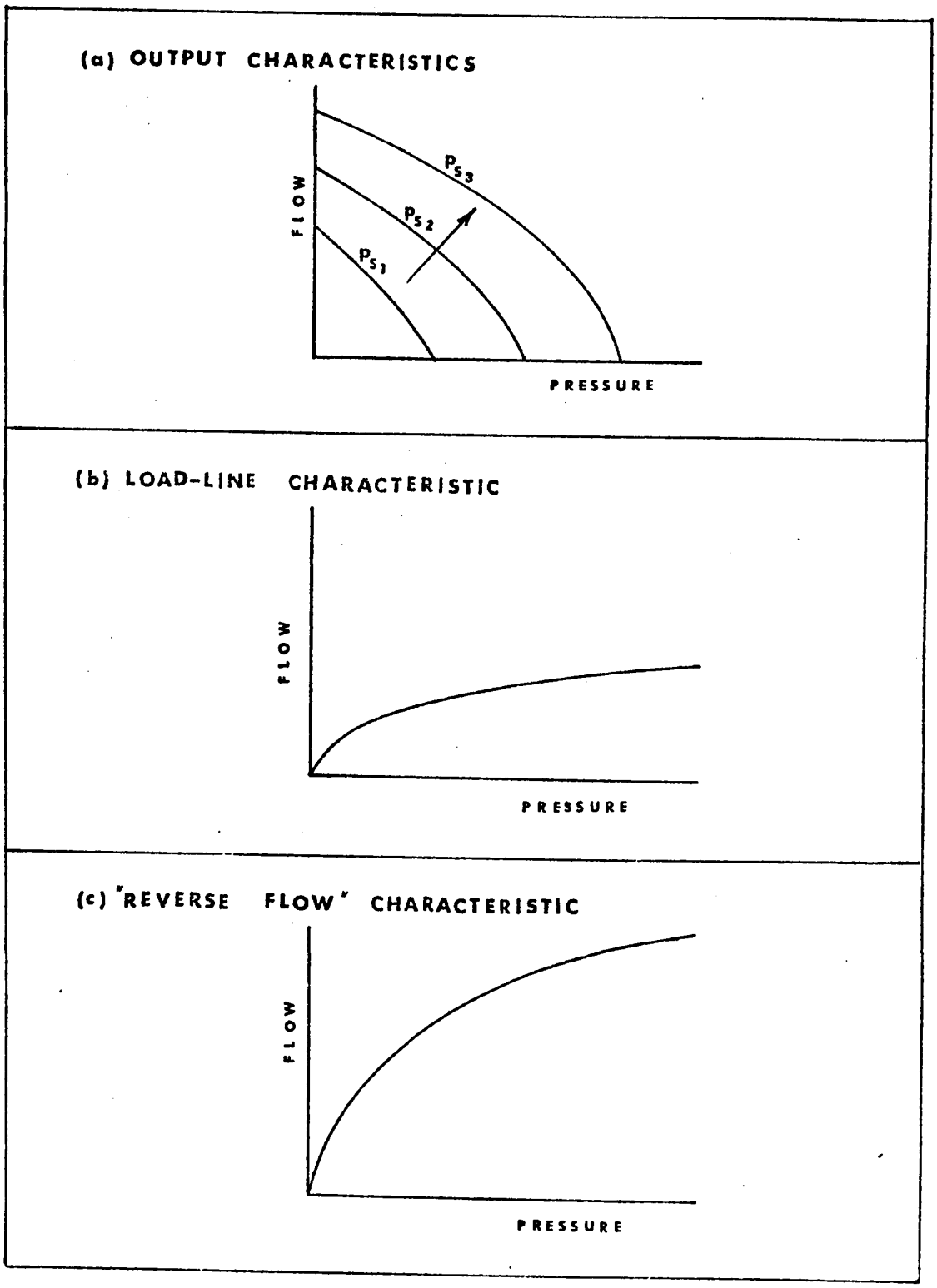

Figure 3. TYPICAL FLUID AMPLIFIER OFERATIONAL CHARACTERISTICS.

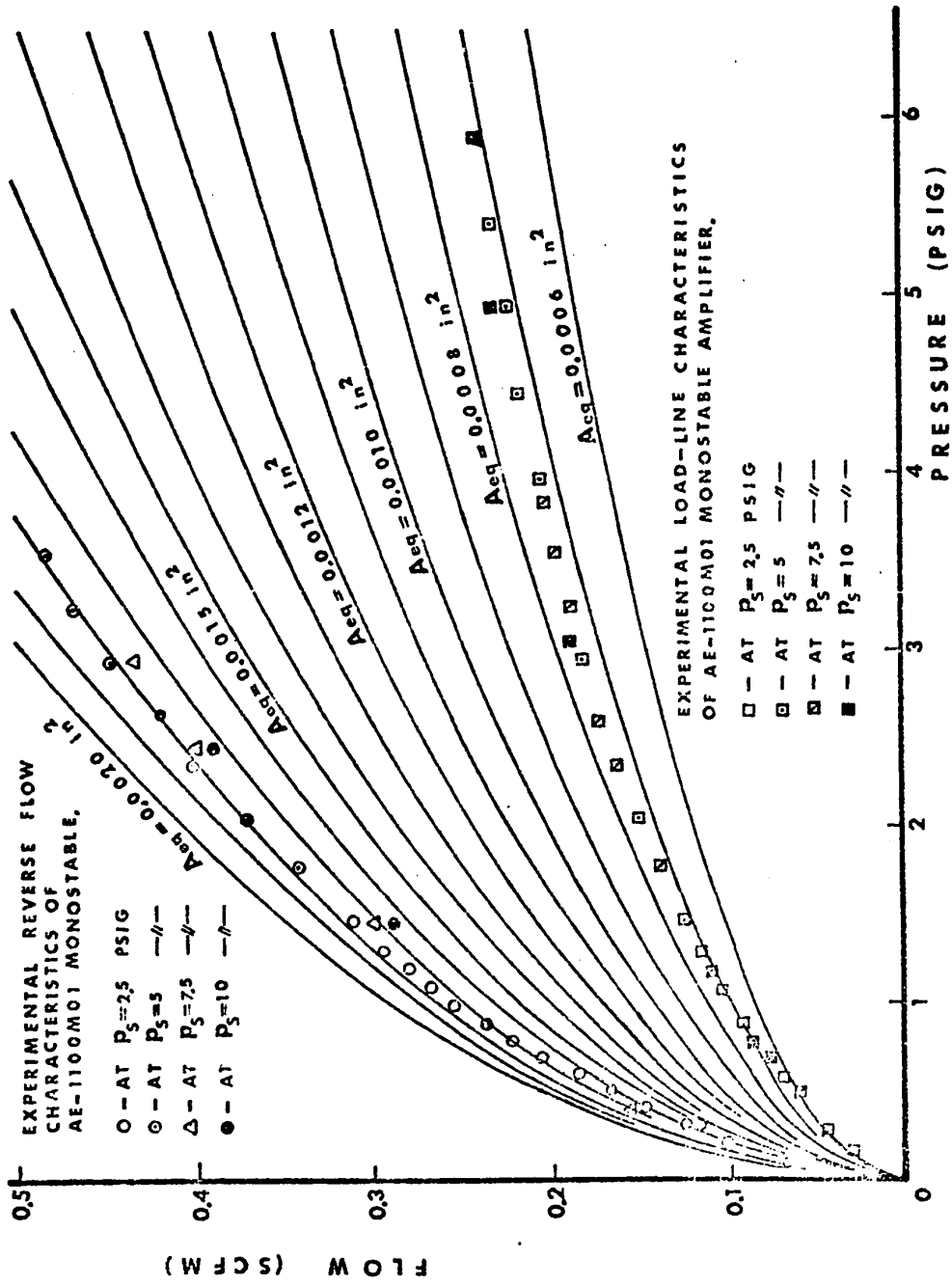

Figure 4. ORIFICE CHARACTERISTICS.

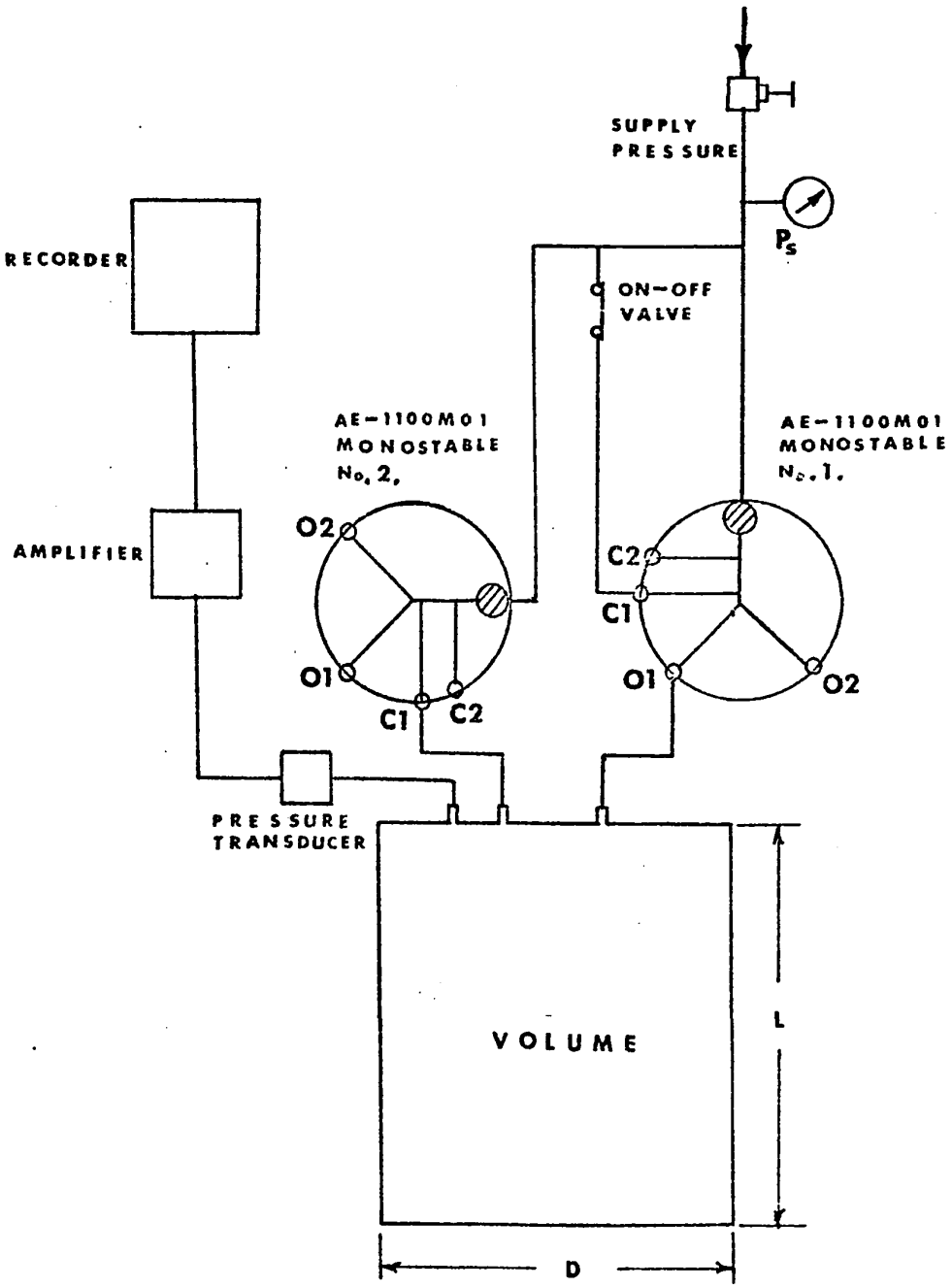

Figure 5. SCHEMATIC OF EXPERIMENTAL SET UP.

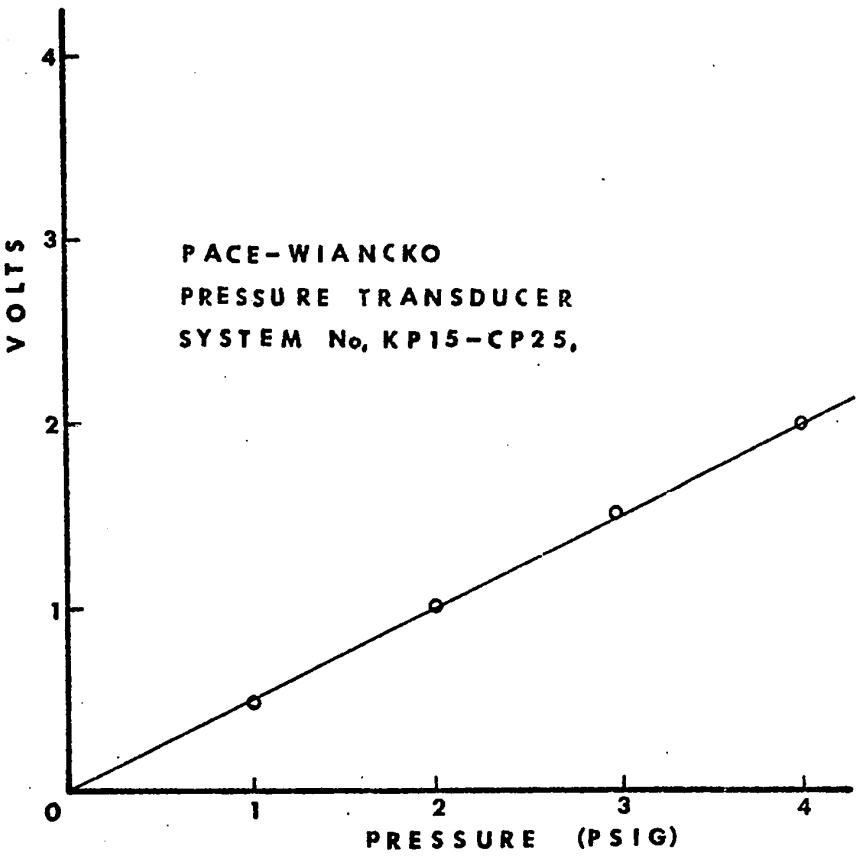

Figure 6. CALIBRATION OF PRESSURE TRANSDUCER.

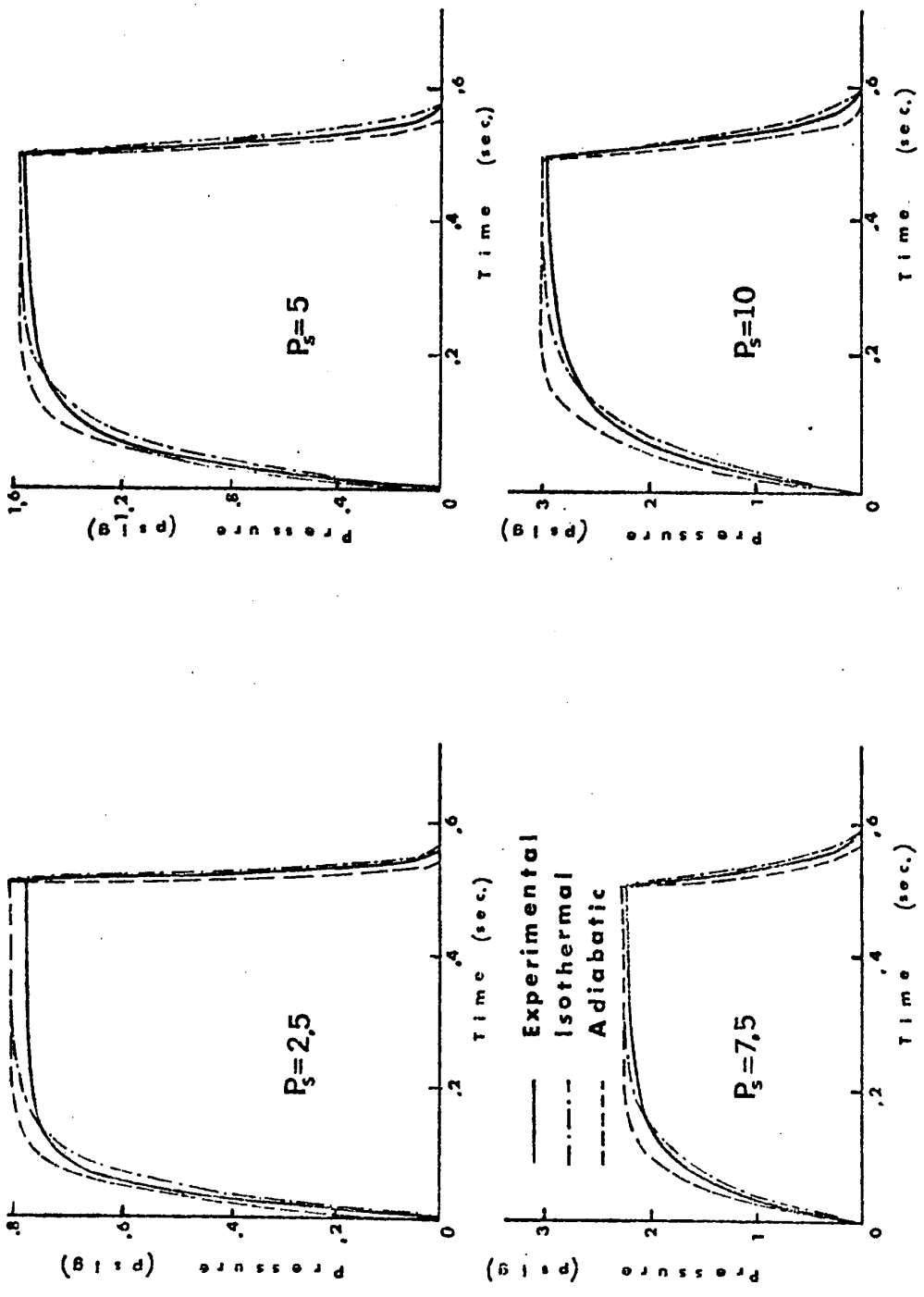

Figure 7. PRESSURE-TIME CHARACTERISTICS. VOLUME No. 1.

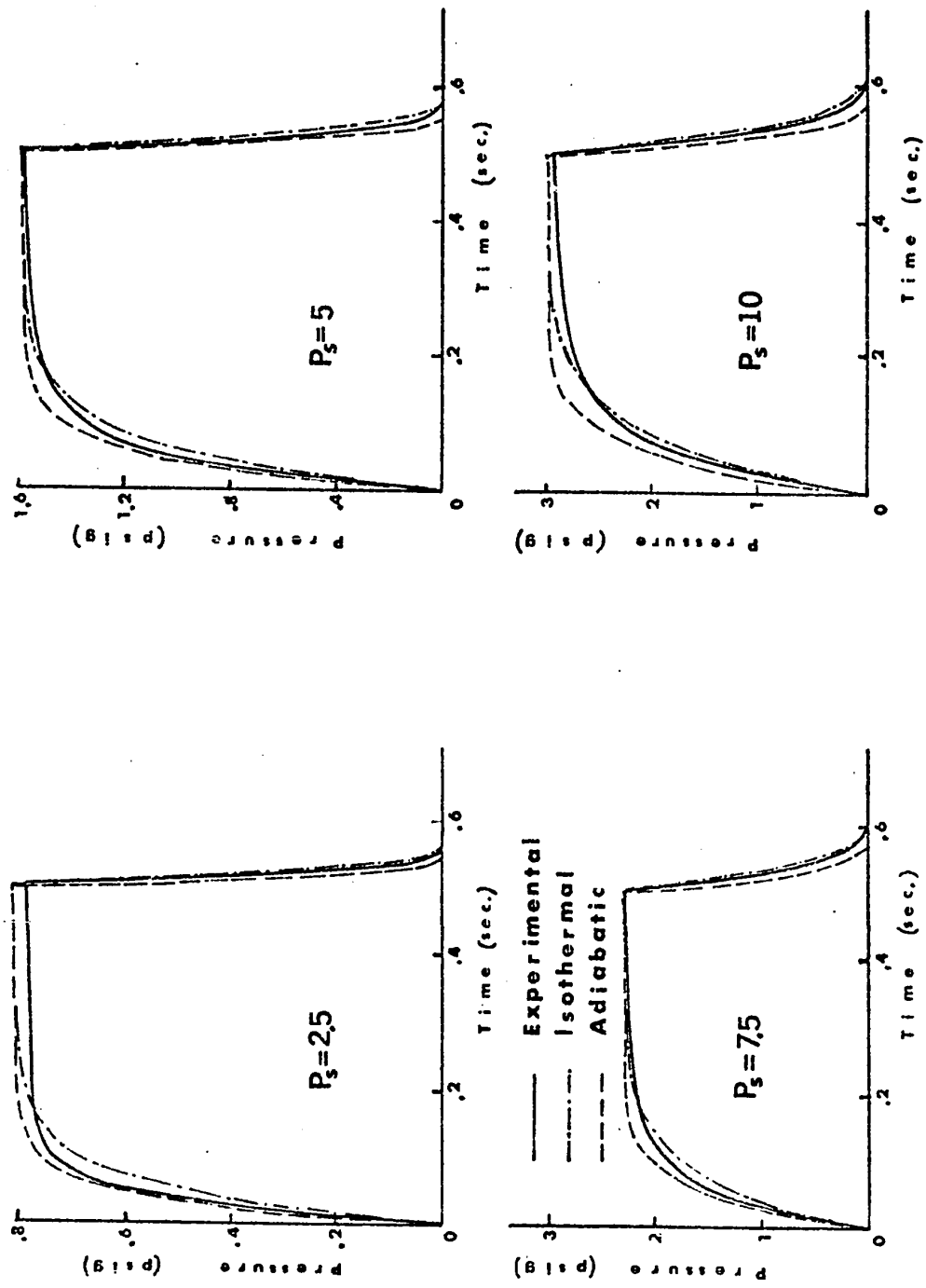

Figure 8. PRESSURE-TIME CHARACTERISTICS. VOLUME No.2.

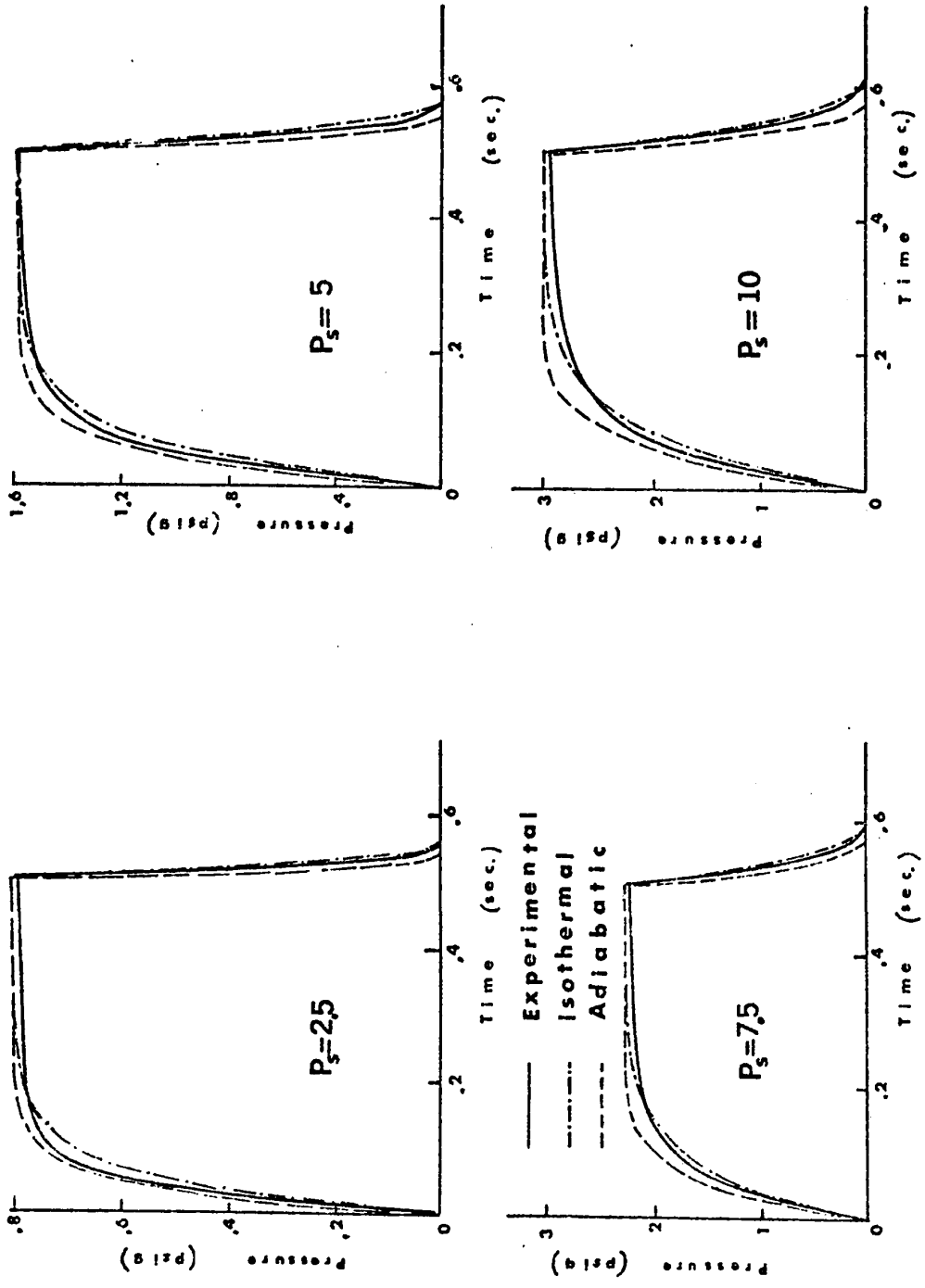

Figure 9. PRESSURE-TIME CHARACTERISTICS. VOLUME No. 3.

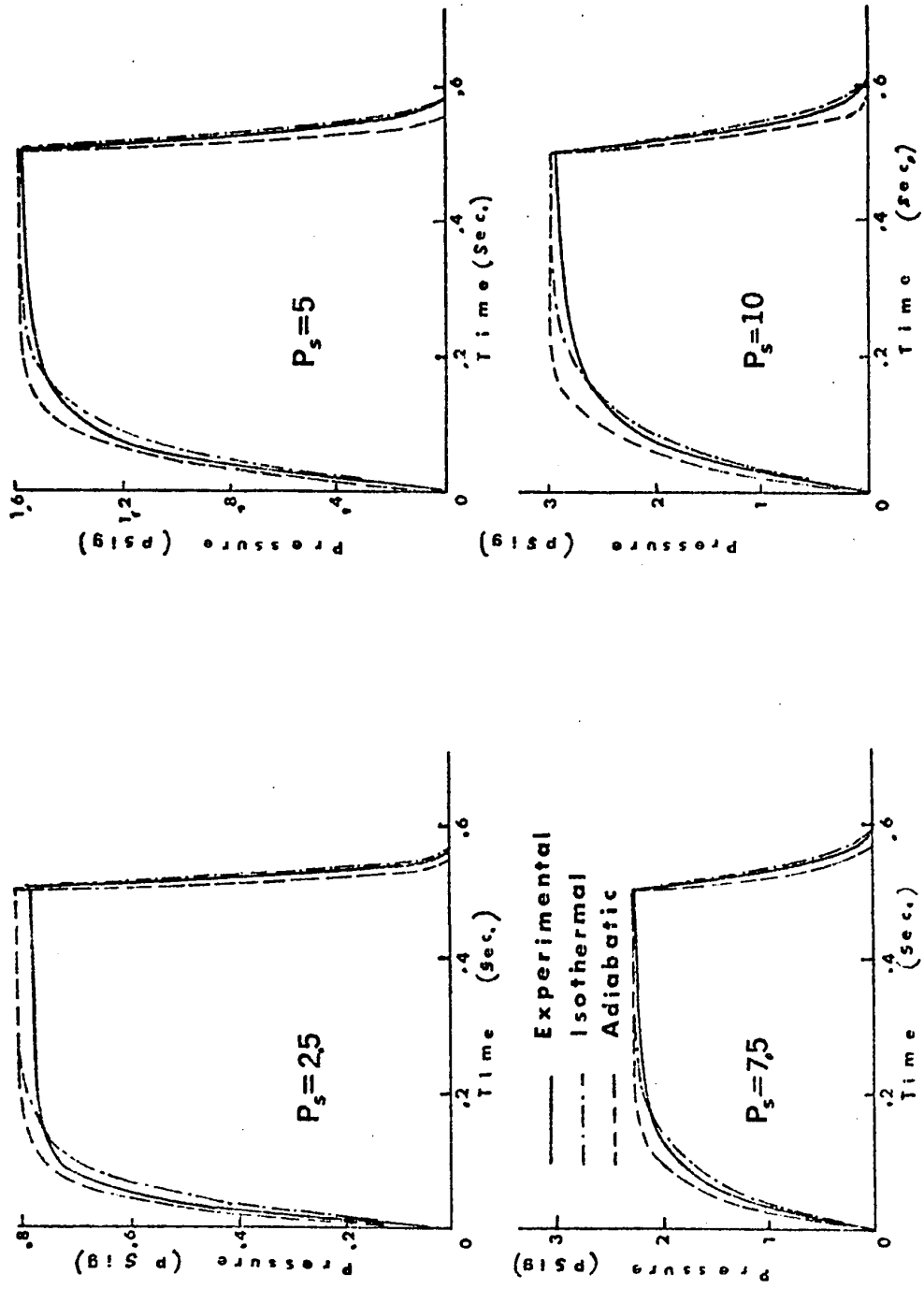

Figure 10. PRESSURE - TIME CHARACTERISTICS. VOLUME No. 4.

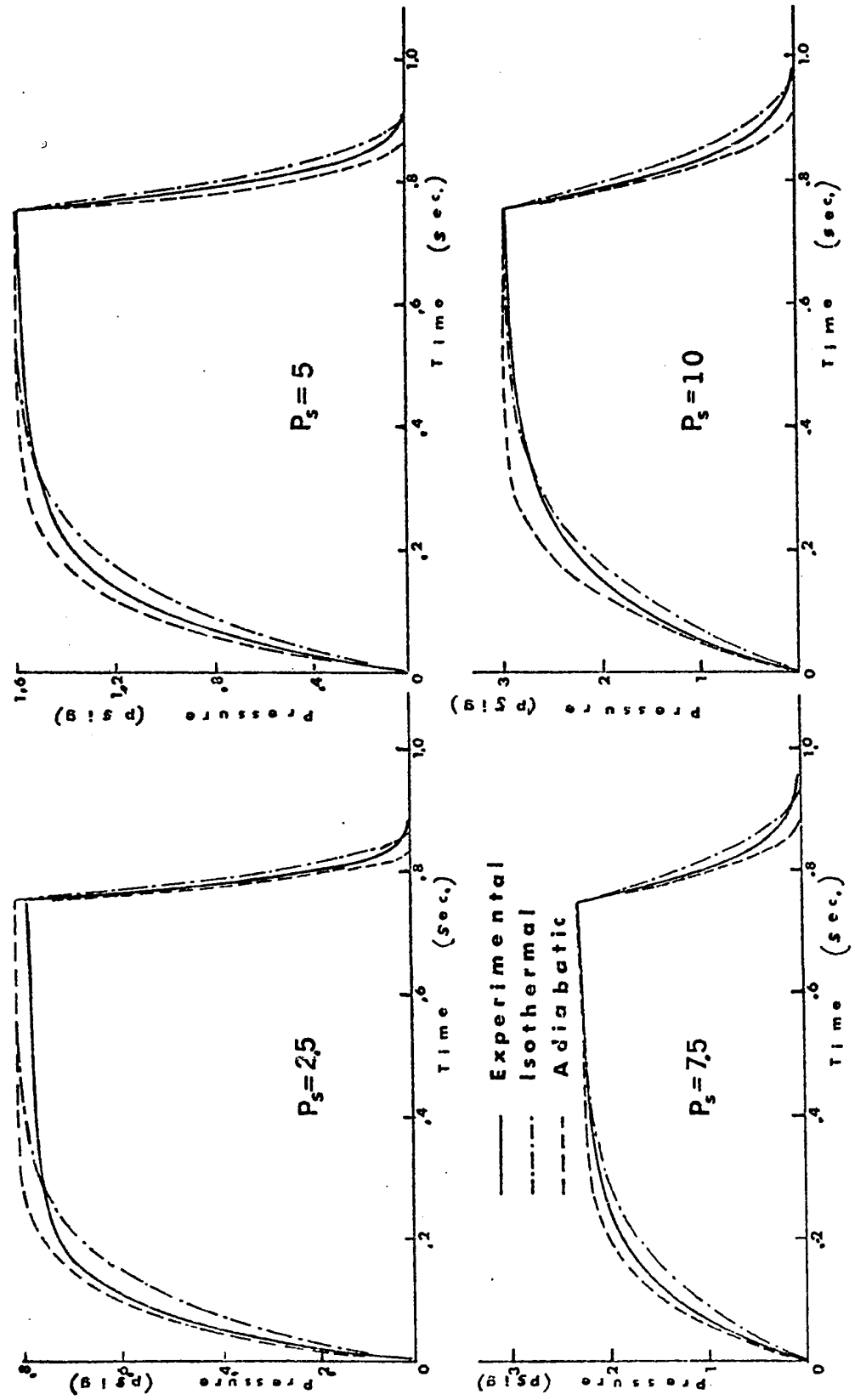

Figure 11. PRESSURE - TIME CHARACTERISTICS. VOLUME No.5.

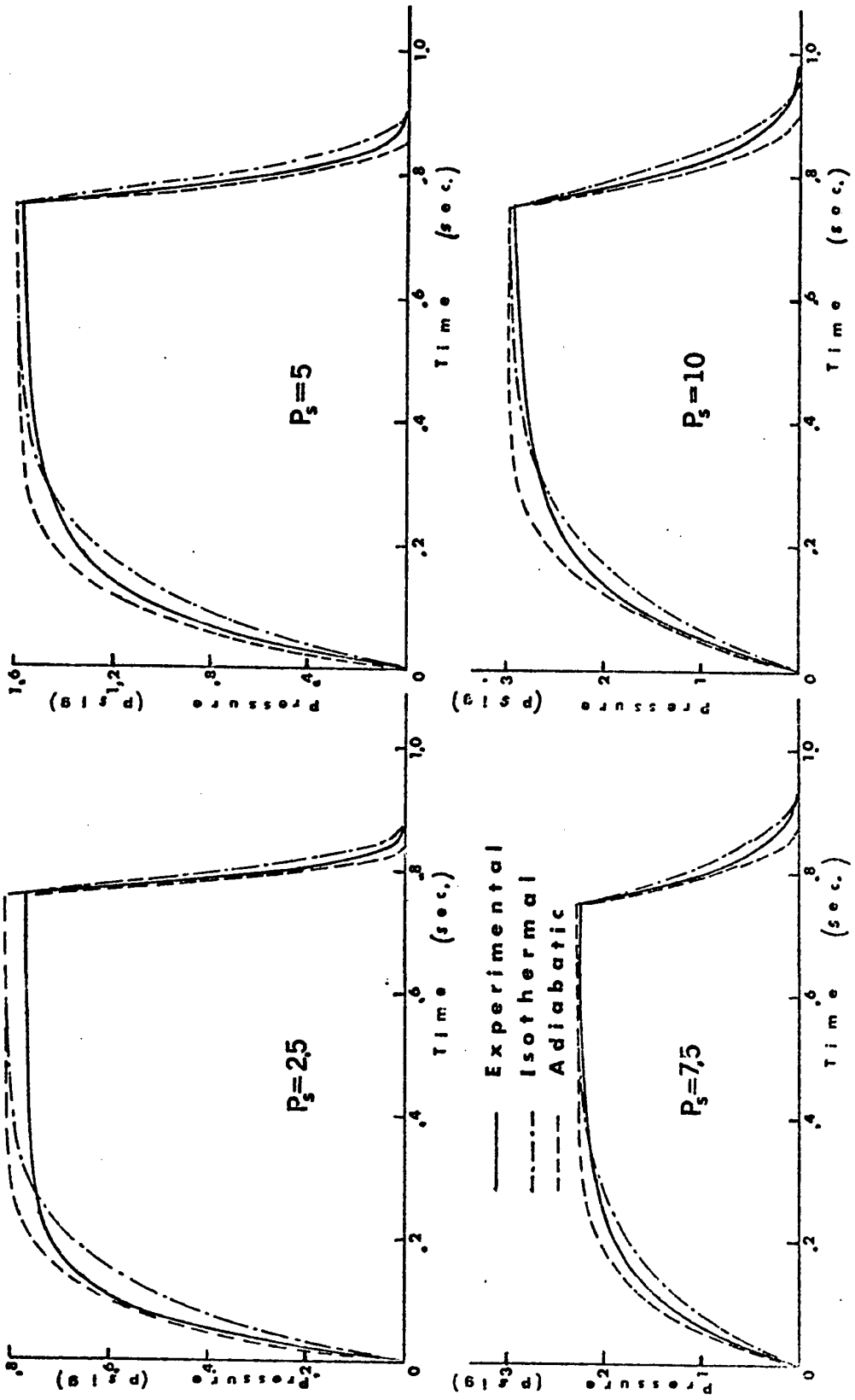

Figure 12. PRESSURE-TIME CHARACTERISTICS. VOLUME No.6.

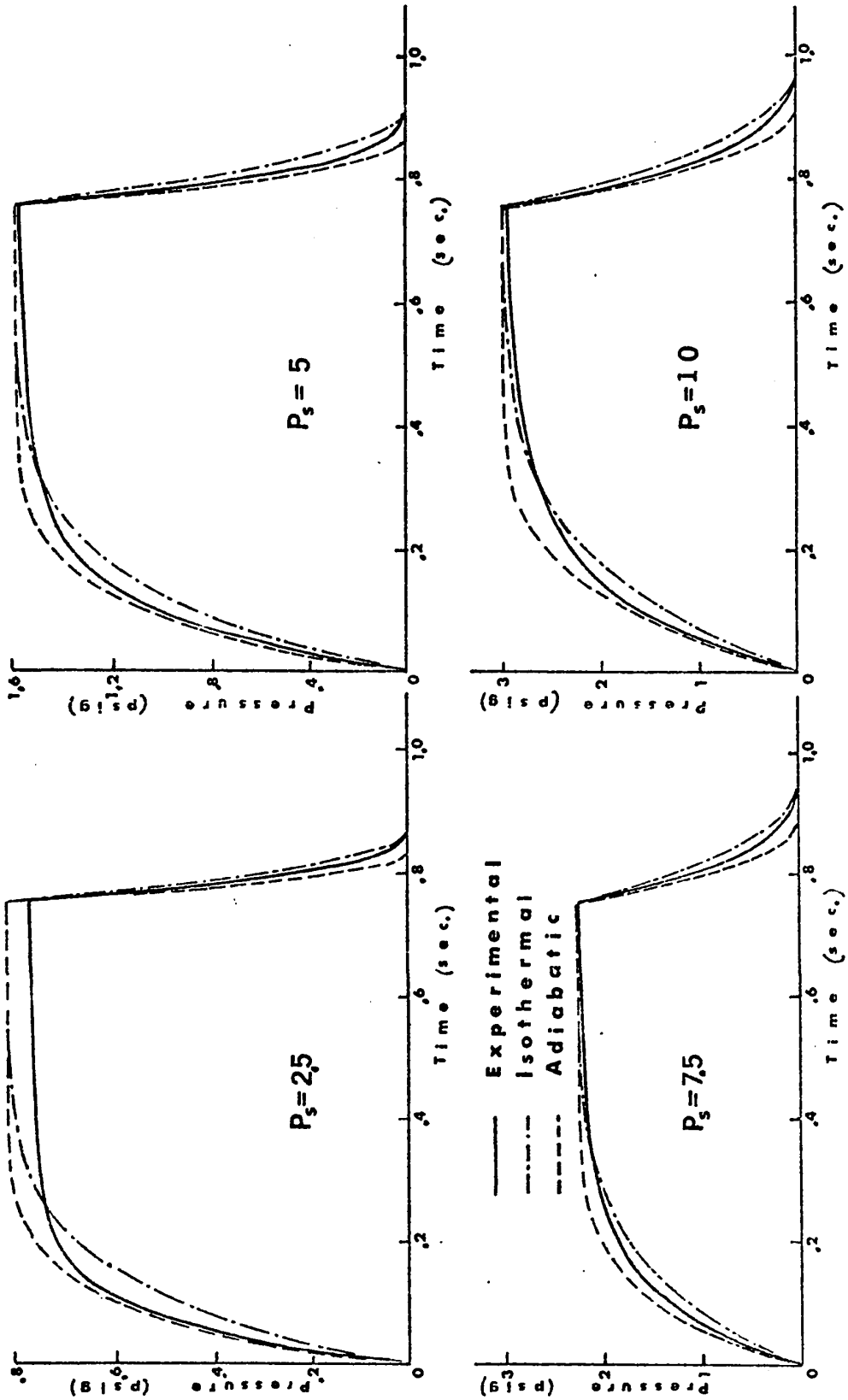

Figure 13. PRSSURE-TIME CHARACTERISTICS. VOLUME No. 7.

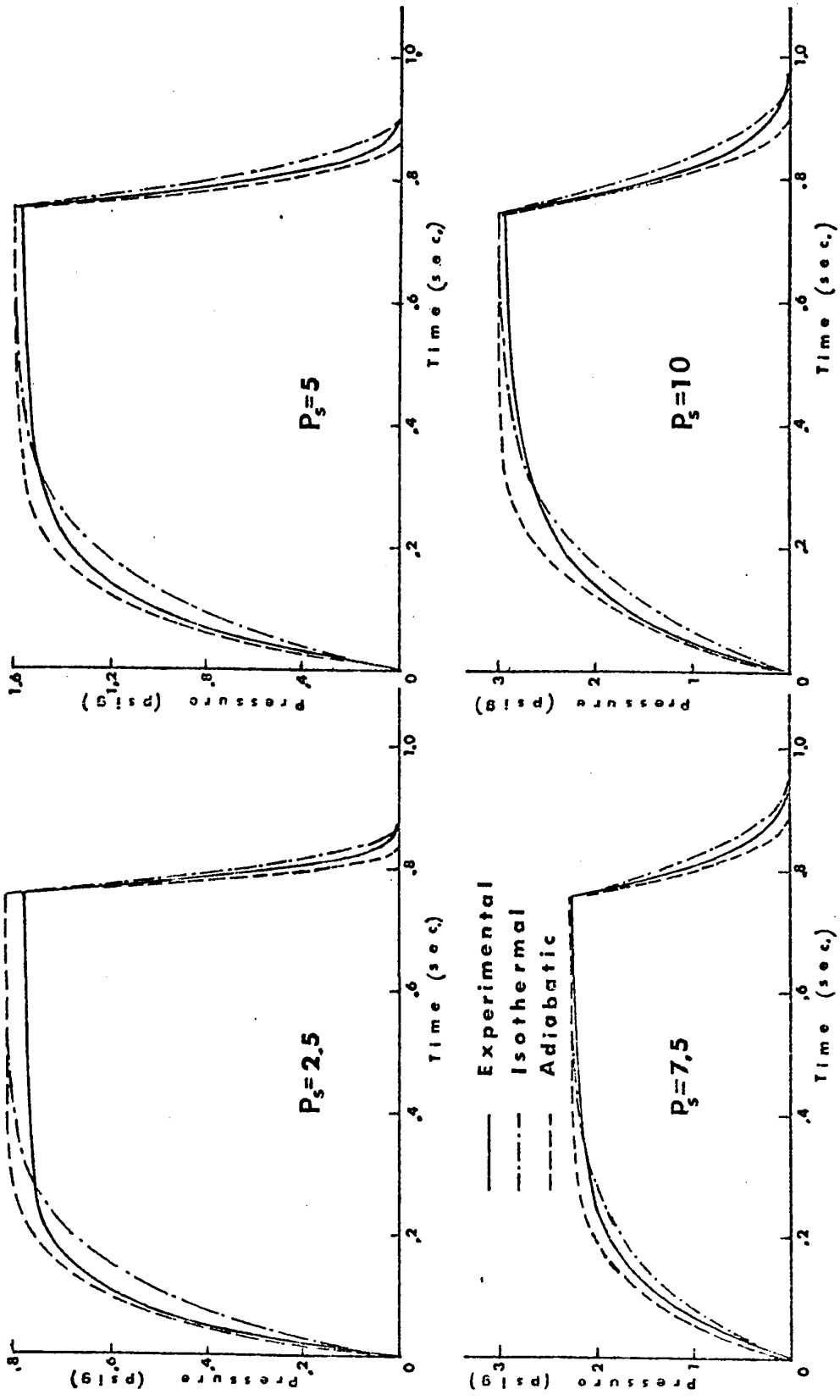

Figure 14. PRESSURE-TIME CHARACTERISTICS, VOLUME No. 8.

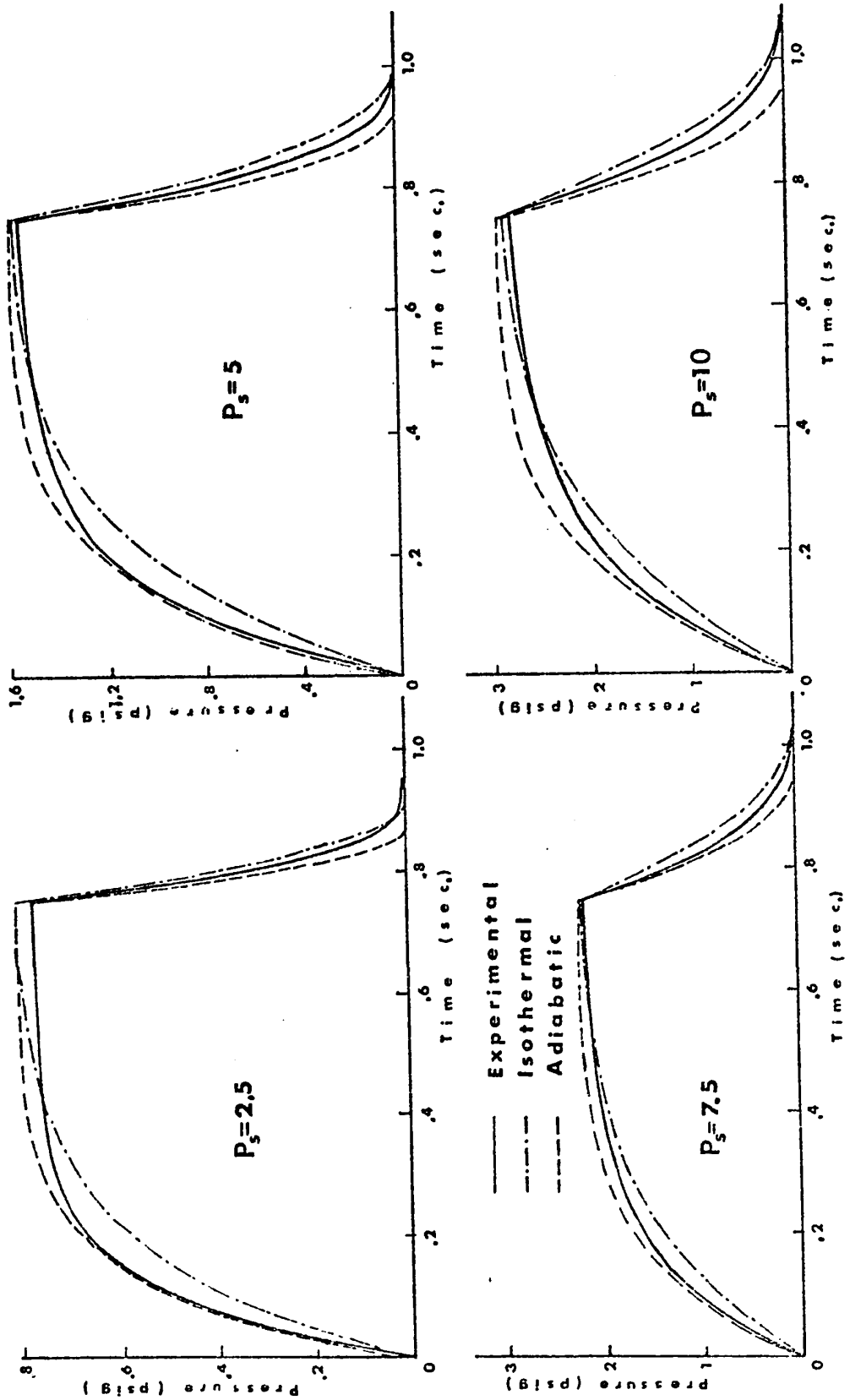

Figure 15. PRESSURE-TIME CHARACTERISTICS. VOLUME No. 9.

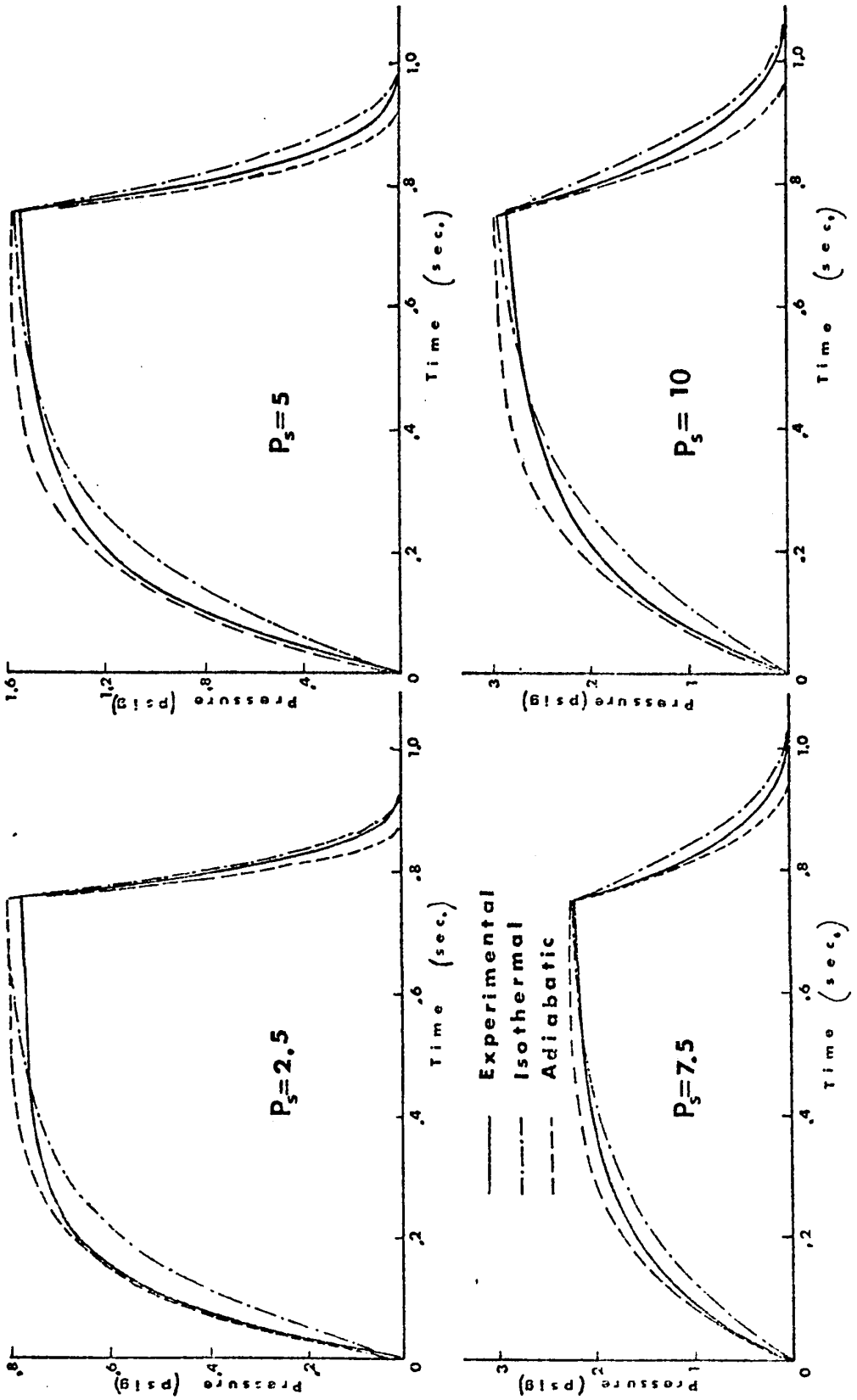

Figure 16. PRESSURE - TIME CHARACTERISTICS. VOLUME No. 10.

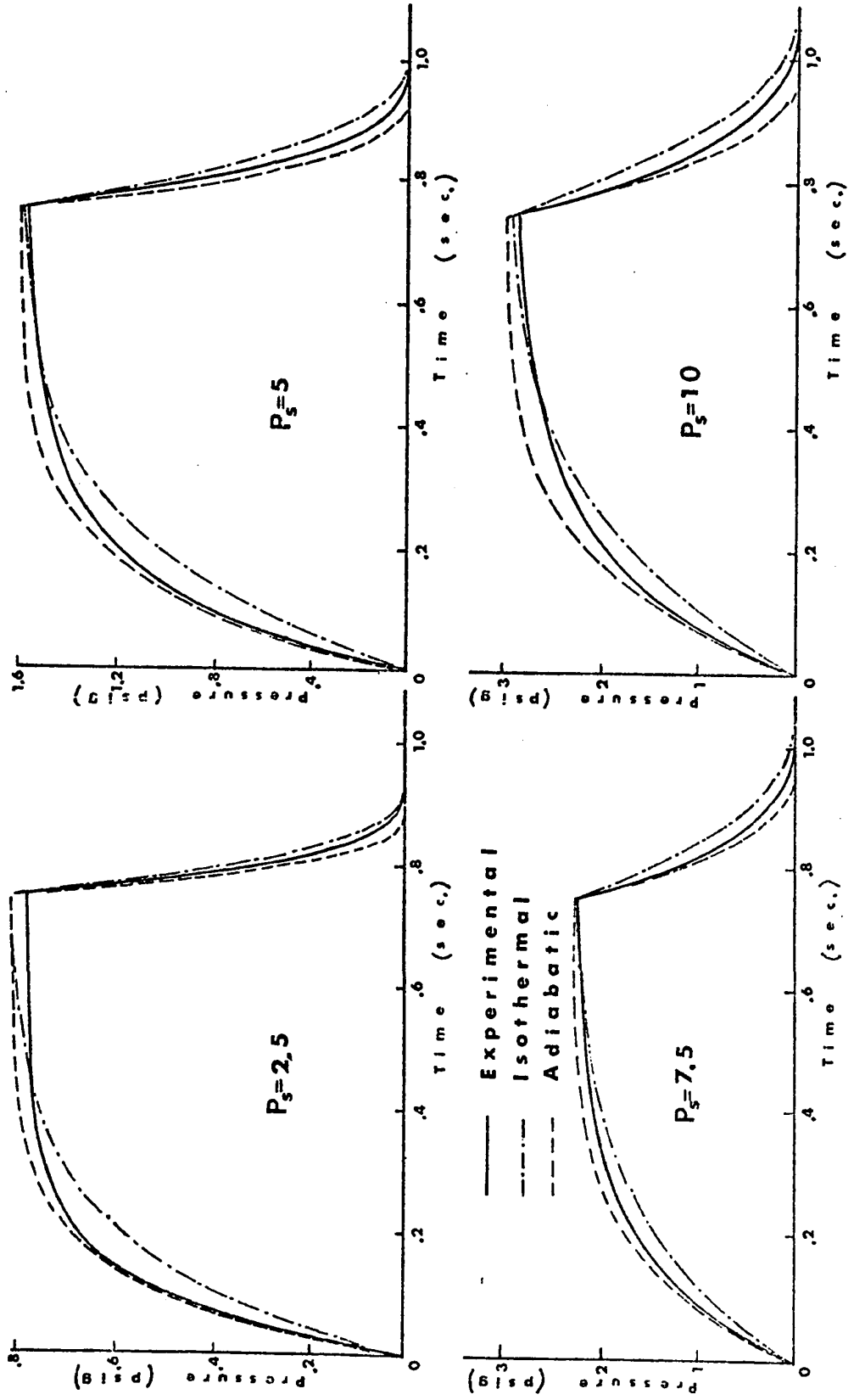

Figure 17. PRESSURE-TIME CHARACTERISTICS. VOLUME No. 11.

REFERENCES

1. Ahrendt, W.R. and Taplin, J.R. Automatic Feedback Control, McGraw-Hill, New York (1951) pp. 271-73.

2. Helm, L. Determination of Pneumatic Capacities of Variable Volume: Acta Technica (Budapest), Vol. 22 (1958) pp. 53-60.

3. Zalmanzon, L.A. Components for Pneumatic Control Instruments, Pergamon Press, London (1965).

4. Zalmanzon, L.A. Fundamentals of Theory and Design of Elements of Pneumo-Automatics: published in "Pneumatic Components and Computing Devices for Control Systems" Butterworths, London (1963).

5. Letham, D.L. Fluidic System Design: Machine Design, Penton Publications, Vol. 38, 7 (1966) pp. 170-181.

6. Kirshner, J.M. Fluid Amplifiers, McGraw-Hill Book Co., New York (1966) pp. 146-186.

7. Woodson, C.W. AC Fluidics: Western Electronic Show and Convention, Los Angeles, California, August 1968.

8. Humphrey, R.L. and Manion, F.M. Low-Pass Filters for Pneumatic Amplifiers: Proc. of the Fluid Amplification Symposium, Vol. 1, Harry Diamond Laboratories, Washington, D.C. May 1964.

9. Hind, E.C. and Hahn, E.J. The Transfer Function of the Pneumatic Capacitance, ASME Paper 65-WA/AUT-18, 1965.

10. Taplin, L.B. and Seleno, A.A. Small-Signal Analysis of Fluidic Circuits, NFPA Fluidic Seminar on Analog Devices, Milwaukee, Wisconsin, November 1966.

11. Andersen, B.W. The Analysis and Design of Pneumatic Systems, John Wiley and Sons, Inc., New York (1967).

12. Krishnaiyer, R. and Lechner, T.J. Jr. An Experimental Evaluation of Fluidic Transmission Line Theory, Advances in Fluidics, The American Society of Mechanical Engineers, New York (1967).

13. Shapiro, A. The Dynamics and Thermodynamics of Compressible Fluid Flow, The Ronald Press Co., New York, Vol. 1 (1953) pp. 73-111.

APPENDIX I

FILE CATALOGUE: Fluidic Components
SECTION: Application Data I-1
TYPE: 1100MO1

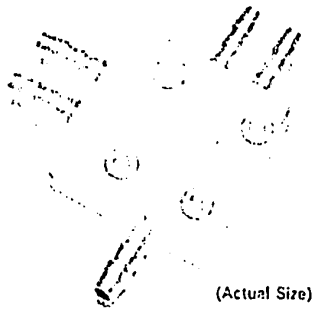
(Actual Size)

MONOSTABLE FLUID AMPLIFIER

DESCRIPTION

The Aviation Electric type 1100MO1 Monostable Fluid Amplifier is a two-input wall attachment digital control element that operates with air and most other commonly used gases. The unit provides the "or/nor" function required in digital control circuitry. The unique method of venting (patent pending) eliminates the impedance matching and rarefaction switching problems usually associated with no-moving-parts fluid amplifiers and permits the straightforward design of pneumatic circuitry using standard off-the-shelf components.

OPERATING CHARACTERISTICS

Function: Two-input Monostable Flip-Flop

Operating Medium: Gaseous Fluids

Operating Principle: Wall Attachment

Temperature Range: −140°F to +270°F.

	MAXIMUM	NOMINAL	MINIMUM
Input Pressure	15 psig	2.5 psig	1.0 psig (See Fig. 1)
Power Consumption		1.1 watts	
Pressure Recovery (blocked)		42%	
Flow Recovery (unblocked)		125%	
Frequency Response		800 cps	
Response Time		0.0004 sec.	
Switching Pressure		0.35 psi max.	

Loading Capacity: Element is stable with zero inactive leg flow from fully opened to fully blocked conditions on the active leg. (See Fig. 2)

Note: Detailed operating characteristics given on the reverse side of this data sheet.

APPLICATIONS

This device has been designed for use in digital and pulse processing fluidic circuits which may be built up in the same way as electronic circuits using solid-state "or/nor" flip-flops. The use of fluidics represents a cost saving and reliability improvement over conventional electronics, and is particularly advantageous in applications where temperature, radiation, shock, vibration, or explosion hazards rule out the choice of electronic/electric circuitry.

SPECIFICATIONS

Dimensions: See drawing on reverse side of sheet

Material: Polycarbonate Thermoplastic

Fittings: Tri-serrated brass suitable for ⅛" I.D. flexible tubing.

Compatibility: Compatible with most common gases, water, oils, acids and alcohols.

Engineering services are available to review applications feasibility.

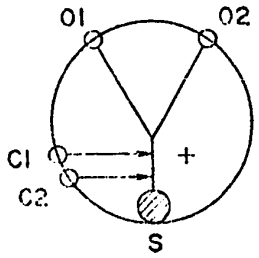

S= SUPPLY

C1 , C2 = INPUTS

$O1 = \overline{C1} \cdot \overline{C2}$ = OUTPUT

O2 = C1 + C2 = OUTPUT

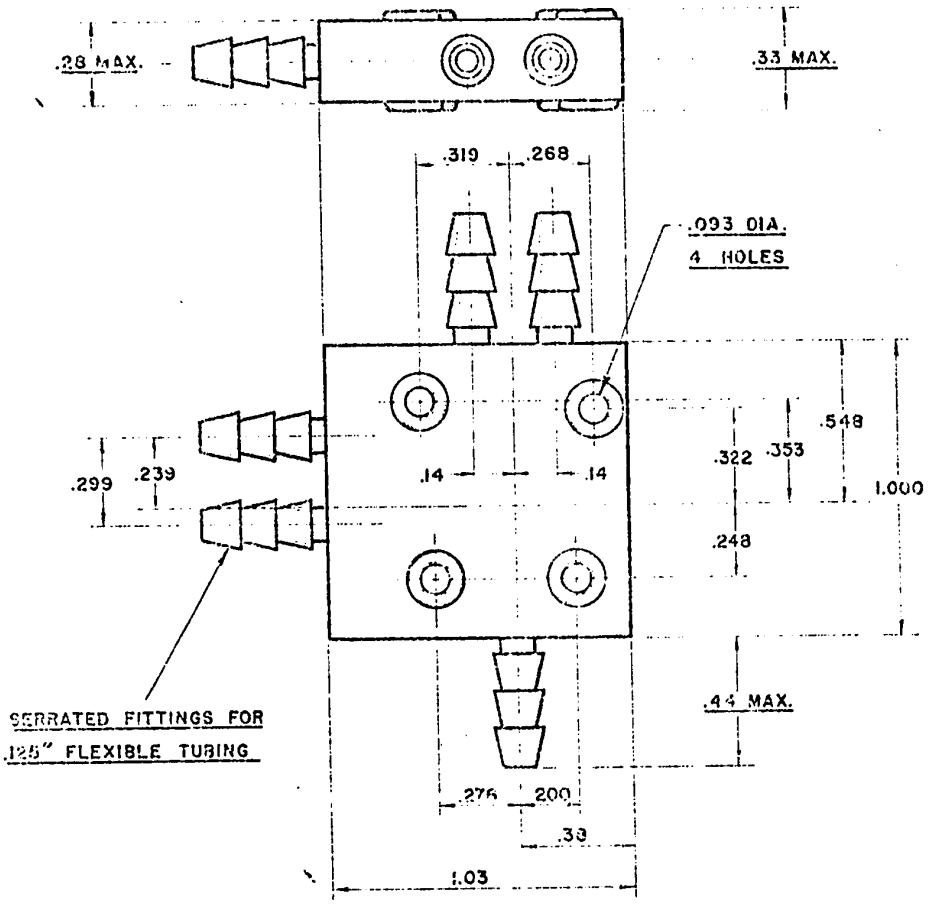

OUTPUT AND LOADLINE CHARACTERISTICS

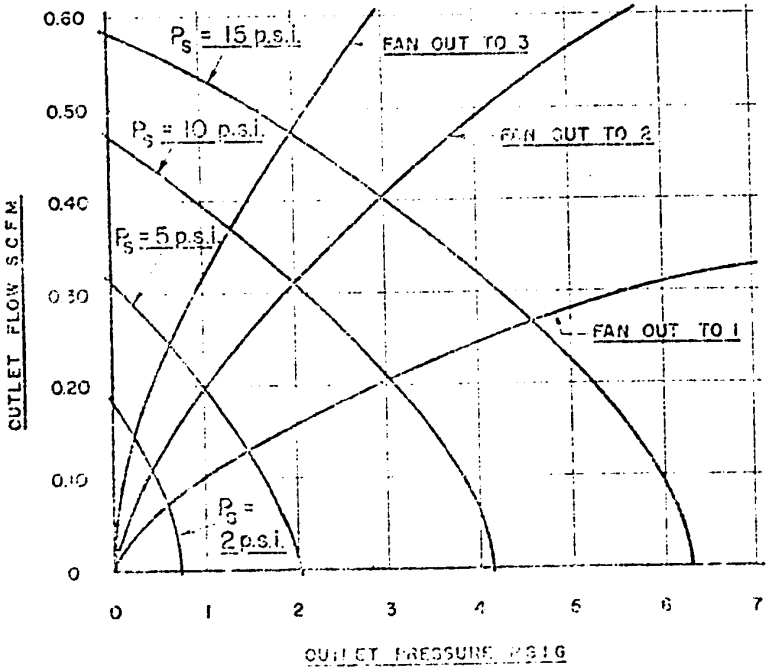

FIGURE 2.

SUPPLY PRESSURE AND FLOW CHARACTERISTICS

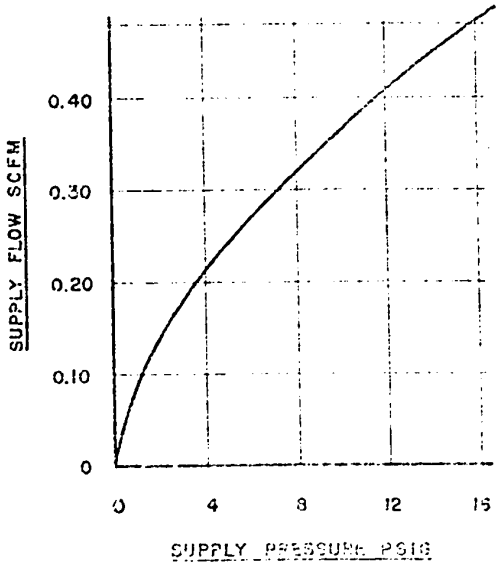

FIGURE 1

```
      PROGRAM JONA
C
C     CONSTANT VOLUME FLUIDIC CAPACITOR.
C
C
      DIMENSION X(4),XDOT(4)
      COMMON CP,AN1,A0,B0,C0,SUB,SUP,P,AN,AM,PA
      EXTERNAL DER
C
 1000 FORMAT(1H1,/,15X,27HFLUIDIC CAPACITOR CHARGING.,//
     1,//,15X,3HPS=,F4.1,10X,2HV=,F4.1,//,15X,2HN=,F3.1,
     2///,15X,4HSEC.,10X,4HPSI.,10X,5HPSIG.,//)
 1001 FORMAT(1H ,F19.3,2F14.3)
 1002 FORMAT(1H1,15X,30HFLUIDIC CAPACITOR DISCHARGING.,//
     1,//,15X,3HPS=,F4.1,10X,2HV=,F4.1,//,15X,2HN=,F3.1,
     2///,15X,4HSEC.,10X,4HPSI.,10X,5HPSIG.,//)
C
      PA=14.7
      TA=459.7+80.
      R=53.3
      ROA=PA*144./(R*TA)
      G=32.2*3600.
      AE1=0.00073
      AE2=0.0018
      AM=1.4
      V=0.
      PS=10.
      DO 30 NV=1,3
      V=V+5.
C
C     PS=10 PSIG.
C     A1, B1, C1 - RELATE TO CHARGING.
C     A2, B2, C2 - RELATE TO DISCHARGING.
C
      A1=-0.0219925
      B1=0.6255212
      C1=-3.9865419
      AN=1.
      DO 40 L=1,5
      X(1)=PA
      DO 13 L1=1,2
      IF(L1-1)14,15,14
   15 A0=A1
      B0=B1
      C0=C1
      AE=AE1
      H=0.0025
      WRITE(61,1000)PS,V,AN
      GO TO 17
   14 A0=0.
      B0=0.
      C0=0.
      AE=AE1+AE2
      H=0.0005
```

```
      WRITE(61,1002)PS,V,AN
   17 CP=AN*PA**(1./AN)/V*28.8
      AN1=(AN-1.)/AN
      SUB=AE/(144.*ROA)*SQRT(2.*AM*G/(R*TA*(AM-1.)))
      SUP=AE/(144.*ROA)*SQRT(AM*G/(R*TA))*(2./(AM+1.))**((AM+1.)
     1/(2.*AM-2.))*(PA*144.)**((AM-1.)/AM)
      P=PA*((AM+1.)/2.)**(AM/(AM-1.))
      T=0.
      K=0
      N=1
      DO 12 I=1,400
      CALL INT(X,XDOT,N,H,T,DER)
      K=K+1
      IF(K-10)12,11,11
   11 K=0
      IF(X(1)-PA)13,10,10
   10 PG=X(1)-PA
      WRITE(61,1001)T,X(1),PG
   12 CONTINUE
   13 CONTINUE
      AN=AN+0.1
   40 CONTINUE
   30 CONTINUE
      STOP
      END
```

FORTRAN DIAGNOSTIC RESULTS FOR JONA

NO ERRORS

JONA P 00723 C 00026 D 00000

```
C
      SUBROUTINE DER(X,XDOT,T,N)
      DIMENSION X(4),XDOT(4)
      COMMON CP,AN1,A0,B0,C0,SUB,SUP,P,AN,AM,PA
      IF(X(1)-P)2,1,1
    1 XDOT(1)=CP*X(1)**AN1*(A0*X(1)**2+B0*X(1)+C0-
     1SUP*(X(1)*144.)**(1./AM))
      GO TO 3
    2 XDOT(1)=CP*X(1)**AN1*(A0*X(1)**2+B0*X(1)+C0-
     1SUB*X(1)*144.*SQRT(ABS((PA/X(1))**((AM+1.)/AM)-(PA/X(1))**2)))
    3 RETURN
      END
```

FORTRAN DIAGNOSTIC RESULTS FOR DER

NO ERRORS

DER P 00204 C 00026 D 00000

```
C
C
      SUBROUTINE INT(X,XDOT,N,H,T,DER)
      DIMENSION X(4),XDOT(4),A(4),B(4),C(4),D(4),TEMP(4),DELTA(4)
      CALL DER(X,XDOT,T,N)
      DO 20 I=1,N
      A(I)=H*XDOT(I)
   20 TEMP(I)=A(I)*0.5+X(I)
      CALL DER(TEMP,XDOT,T+H/2.,N)
      DO 21 I=1,N
      B(I)=H*XDOT(I)
   21 TEMP(I)=X(I)+B(I)*0.5
      CALL DER(TEMP,XDOT,T+H/2.,N)
      DO 22 I=1,N
      C(I)=H*XDOT(I)
   22 TEMP(I)=C(I)+X(I)
      CALL DER(TEMP,XDOT,T+H,N)
      DO 23 I=1,N
   23 D(I)=H*XDOT(I)
      DO 24 I=1,N
      DELTA(I)=1./6.*(A(I)+2.*B(I)+2.*C(I)+D(I))
   24 X(I)=X(I)+DELTA(I)
      T=T+H
      RETURN
      END
```

FORTRAN DIAGNOSTIC RESULTS FOR INT

NO ERRORS

```
   INT          P   00427   C   00000   D   00000
OBJ,LGO
```


FLUIDIC CAPACITOR CHARGING.

PS=10.0 V= 5.0

N=1.0

SEC.	PSI.	PSIG.
.025	15.498	.798
.050	16.116	1.416
.075	16.589	1.889
.100	16.940	2.240
.125	17.195	2.495
.150	17.375	2.675
.175	17.502	2.802
.200	17.589	2.889
.225	17.650	2.950
.250	17.691	2.991
.275	17.719	3.019
.300	17.738	3.038
.325	17.751	3.051
.350	17.760	3.060
.375	17.766	3.066
.400	17.770	3.070
.425	17.773	3.073
.450	17.775	3.075
.475	17.776	3.076
.500	17.777	3.077
.525	17.777	3.077
.550	17.778	3.078
.575	17.778	3.078
.600	17.778	3.078
.625	17.778	3.078
.650	17.778	3.078
.675	17.778	3.078
.700	17.778	3.078
.725	17.778	3.078
.750	17.778	3.078
.775	17.778	3.078
.800	17.778	3.078
.825	17.779	3.079
.850	17.779	3.079
.875	17.779	3.079
.900	17.779	3.079
.925	17.779	3.079
.950	17.779	3.079
.975	17.779	3.079
1.000	17.779	3.079

PS=10.0 V= 5.0

N=1.0

SEC.	PSI.	PSIG.
.005	17.515	2.815
.010	17.264	2.564
.015	17.023	2.323
.020	16.793	2.093
.025	16.575	1.875
.030	16.369	1.669
.035	16.174	1.474
.040	15.991	1.291
.045	15.819	1.119
.050	15.660	.960
.055	15.512	.812
.060	15.377	.677
.065	15.254	.554
.070	15.143	.443
.075	15.044	.344
.080	14.958	.258
.085	14.884	.184
.090	14.822	.122
.095	14.773	.073
.100	14.737	.037
.105	14.713	.013
.110	14.701	.001

FLUIDIC CAPACITOR CHARGING.

PS=10.0 V= 5.0

N=1.4

SEC.	PSI.	PSIG.
.025	15.774	1.074
.050	16.528	1.828
.075	17.028	2.328
.100	17.340	2.640
.125	17.526	2.826
.150	17.635	2.935
.175	17.697	2.997
.200	17.733	3.033
.225	17.753	3.053
.250	17.764	3.064
.275	17.770	3.070
.300	17.774	3.074
.325	17.776	3.076
.350	17.777	3.077
.375	17.778	3.078
.400	17.778	3.078
.425	17.778	3.078
.450	17.778	3.078
.475	17.778	3.078
.500	17.778	3.078
.525	17.778	3.078
.550	17.778	3.078
.575	17.779	3.079
.600	17.779	3.079
.625	17.779	3.079
.650	17.779	3.079
.675	17.779	3.079
.700	17.779	3.079
.725	17.779	3.079
.750	17.779	3.079
.775	17.779	3.079
.800	17.779	3.079
.825	17.779	3.079
.850	17.779	3.079
.875	17.779	3.079
.900	17.779	3.079
.925	17.779	3.079
.950	17.779	3.079
.975	17.779	3.079
1.000	17.779	3.079

PS=10.0 V= 5.0

N=1.4

SEC.	PSI.	PSIG.
.005	17.395	2.695
.010	17.037	2.337
.015	16.706	2.006
.020	16.401	1.701
.025	16.121	1.421
.030	15.867	1.167
.035	15.638	.938
.040	15.434	.734
.045	15.256	.556
.050	15.102	.402
.055	14.973	.273
.060	14.870	.170
.065	14.791	.091
.070	14.736	.036
.075	14.706	.006

APPENDIX III

Determination of the Fluid Amplifier Characteristics

A.3.1. The output characteristics of the fluidic monostable amplifier AE 1100 MO 1 (No. 1)

The pressure-flow characteristic curves for the charging amplifier No. 1 (AE 1100 MO 1) were obtained for its output leg "01" which is a normally active output port for the monostable amplifier. This output is used later to connect the amplifier with the input of the capacitor. The pressure-flow characteristics were obtained by gradually loading the output port 01 and then measuring the instantaneous pressure upstream of the load and the flow recoveries at the exit. A schematic of the experimental set-up is shown in Fig. A.1(a). This test was repeated for different supply pressures of 2.5, 5, 7.5 and 10 psig. The experimental results are presented in Fig. A.2.

Using the standard curve-fitting technique, the constants A, B and C of eq. (1) were found for the various supply pressures. These values are presented in the following table. From eq.(1), with the above constants, the theoretical pressure-flow characteristic curves were obtained and are plotted in Fig. A.2. It is seen from Fig. A.2 that the curves derived

P_s psig	A	B	C
2.5	0.1008	2.9329	21.1406
5.0	0.0524	1.5188	10.7030
7.5	0.0344	0.9946	6.8000
10.0	0.0220	0.6225	3.9865

fit quite well with the experimental data, except for the case of P_s = 2.5 psig where an approximate error of 10% is realized at the point of maximum pressure recovery.

A.3.2. <u>The "reverse flow" characteristics of the monostable amplifier AE 1100 MO 1 (No. 1)</u>

A schematic of this test set-up is shown in Fig. A.1(b). In order to obtain the reverse flow characteristics through leg "01", one of the control jets must be active so that the output of the amplifier will be diverted to leg "02". This was achieved by switching "on" the "on-off" switch to the control port "C1". The pressure-flow characteristics were obtained by gradually increasing the pressure at 01 and then measuring the instantaneous pressure and flow through the leg 01. Back-pressure corrections were incorporated into the flow meter readings, thus reducing the flow rate to standard cubic feet per minute, scfm. This test was repeated for the four

amplifier supply pressures of 2.5, 5, 7.5 and 10 psig.

The experimental results for the reverse flow characteristics are shown in Fig. 4, where the data are superimposed on the theoretical orifice flow curves plotted for different equivalent flow areas. It is noticeable that the experimental results for the various supply pressures fall on the same curve, which means that these characteristics are independent of the supply pressure of the amplifier. By comparison with the theoretical orifice pressure-flow characteristic curves, the equivalent area "A_{eq_2}", which represents the reverse flow characteristics, was found equal to 0.0018 in^2.

A.3.3. The "load line" pressure flow characteristics of the monostable amplifier AE 1100 MO 1 (No. 2)

The schematic of the experimental set-up is shown in Fig. A.1(c). The amplifier was connected through its supply port to a constant supply pressure. Its control port C1 was connected to another pressure supply via a flowmeter. The load line pressure-flow characteristics were then obtained by gradually increasing the pressure at C1 and then measuring the instantaneous pressure and flow through the control port C1. Errors due to back-pressure effects on the flow meter readings were appropriately corrected. Such tests were repeated for the

four different amplifier supply pressures of 2.5, 5, 7.5 and 10 psig.

The results of these experiments are presented in Fig. 4. Similar to the reverse flow case, it is shown that the load line characteristic is independent of the supply pressure because test data for various supply pressures all fall on one line. By comparison of these results with the theoretical orifice pressure-flow characteristic curves, the equivalent area "A_{eq_1}", representing the load line characteristics, was found equal to 0.00073 in^2.

(a) EVALUATION OF OUTPUT CHARACTERISTICS.

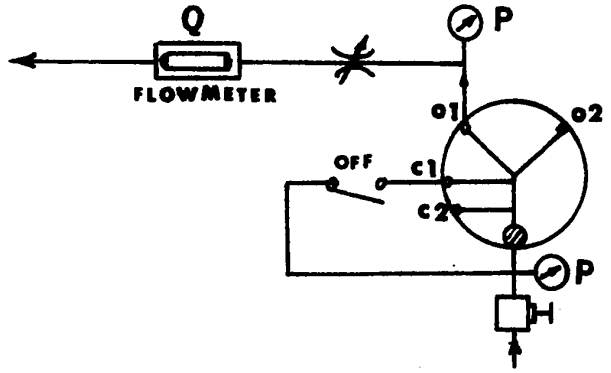

(b) VALUATION OF REVERSE FLOW CHARACTERISTICS.

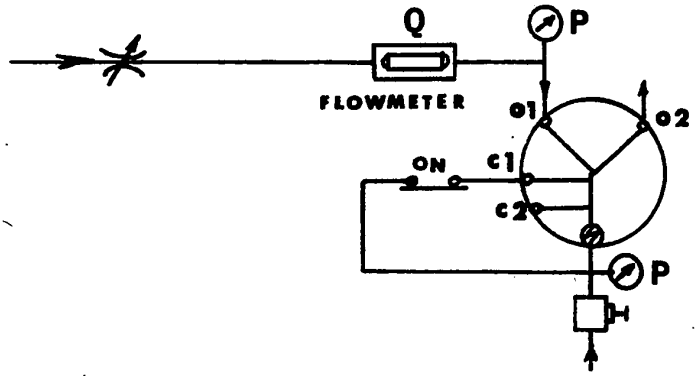

(c) EVALUATION OF LOAD-LINE CHARACTERISTICS.

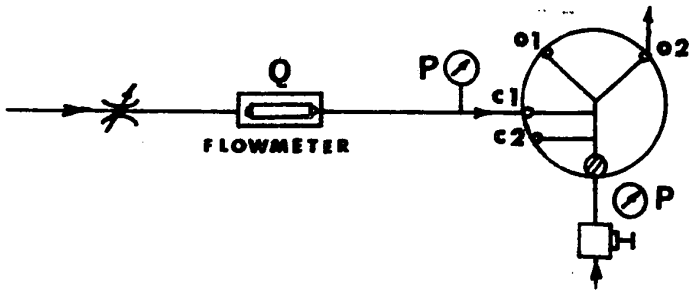

Figure A.1. TEST SET UPS.

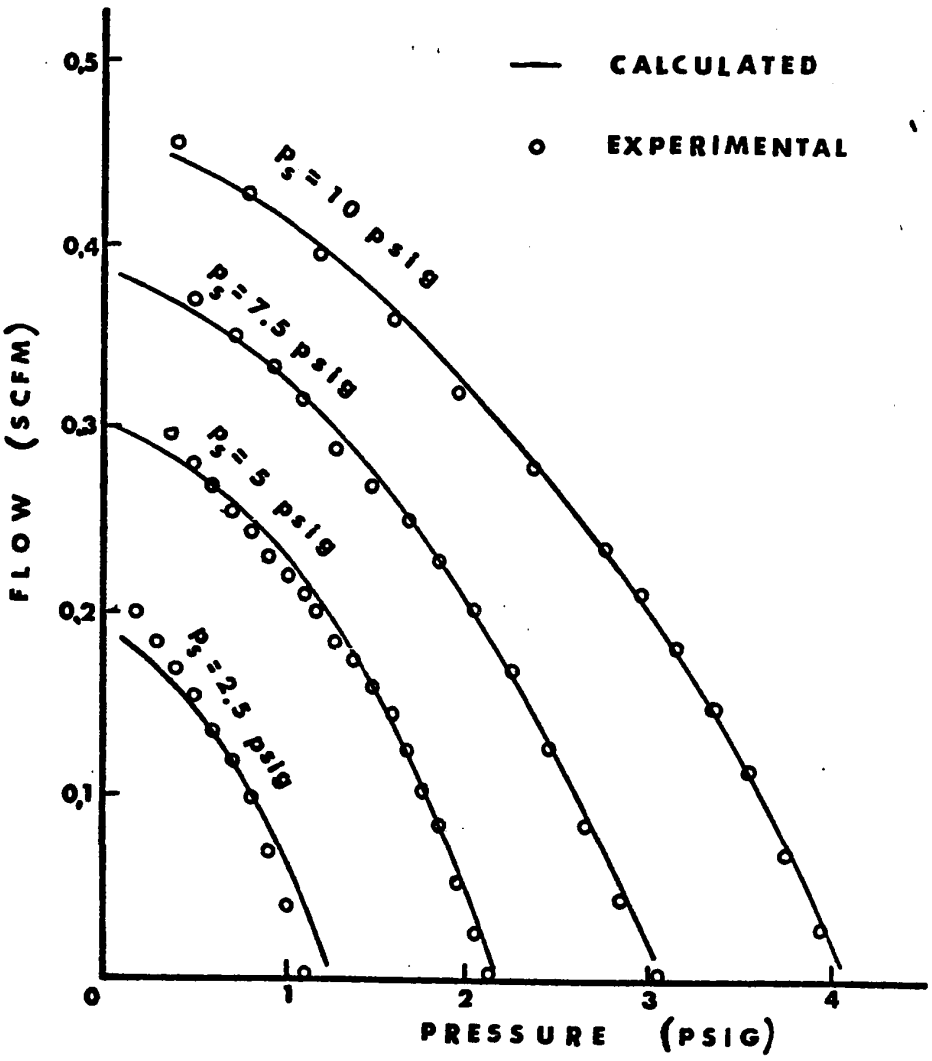

Figure A.2. FLUID AMPLIFIER OUTPUT CHARACTERISTICS.